Lecture 8: Protostars and the Collapse of Rotating Cores

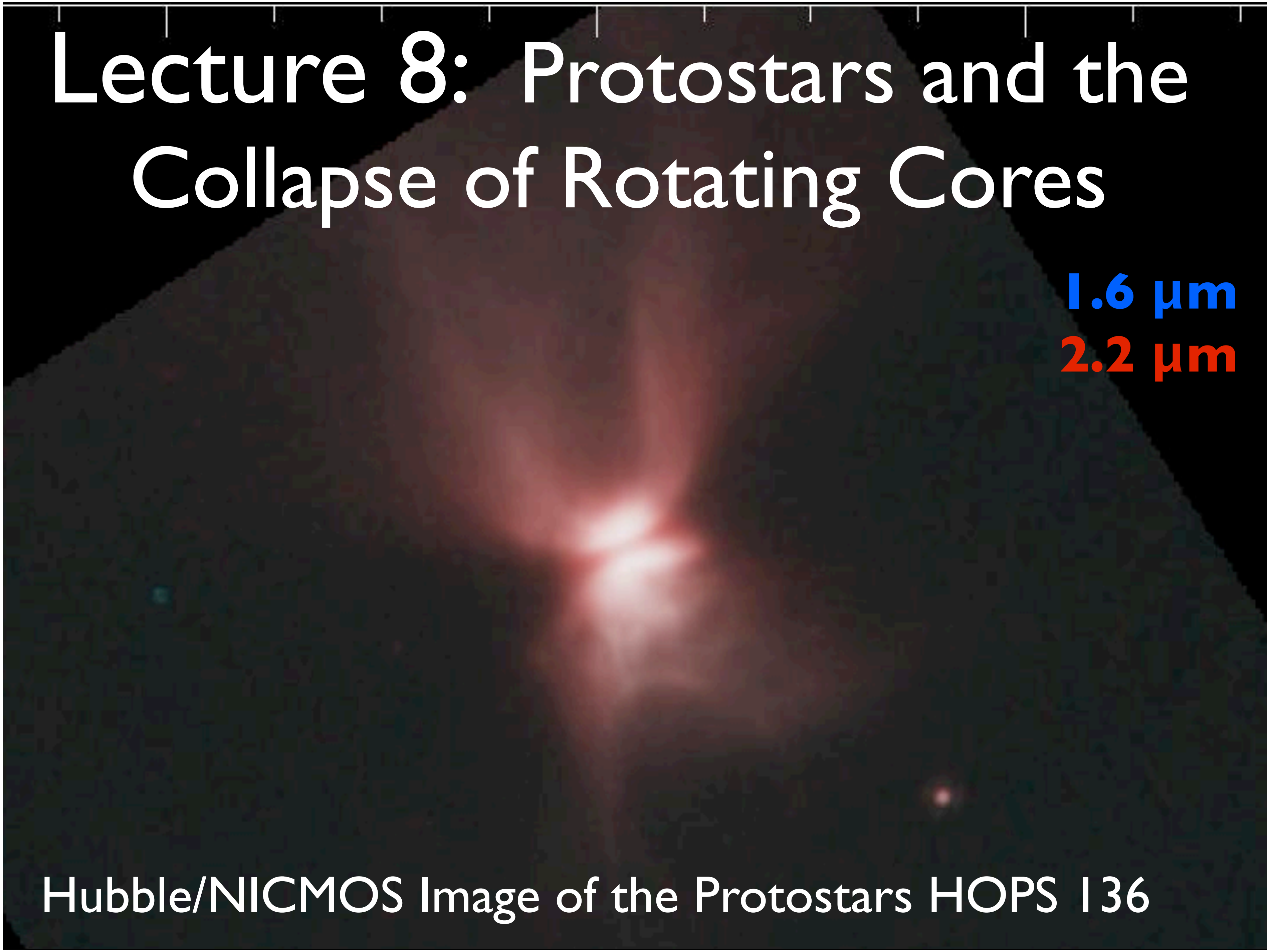

Hubble/NICMOS Image of the Protostars HOPS 136

Most of the Candidates Orbit Stars Like our Sun

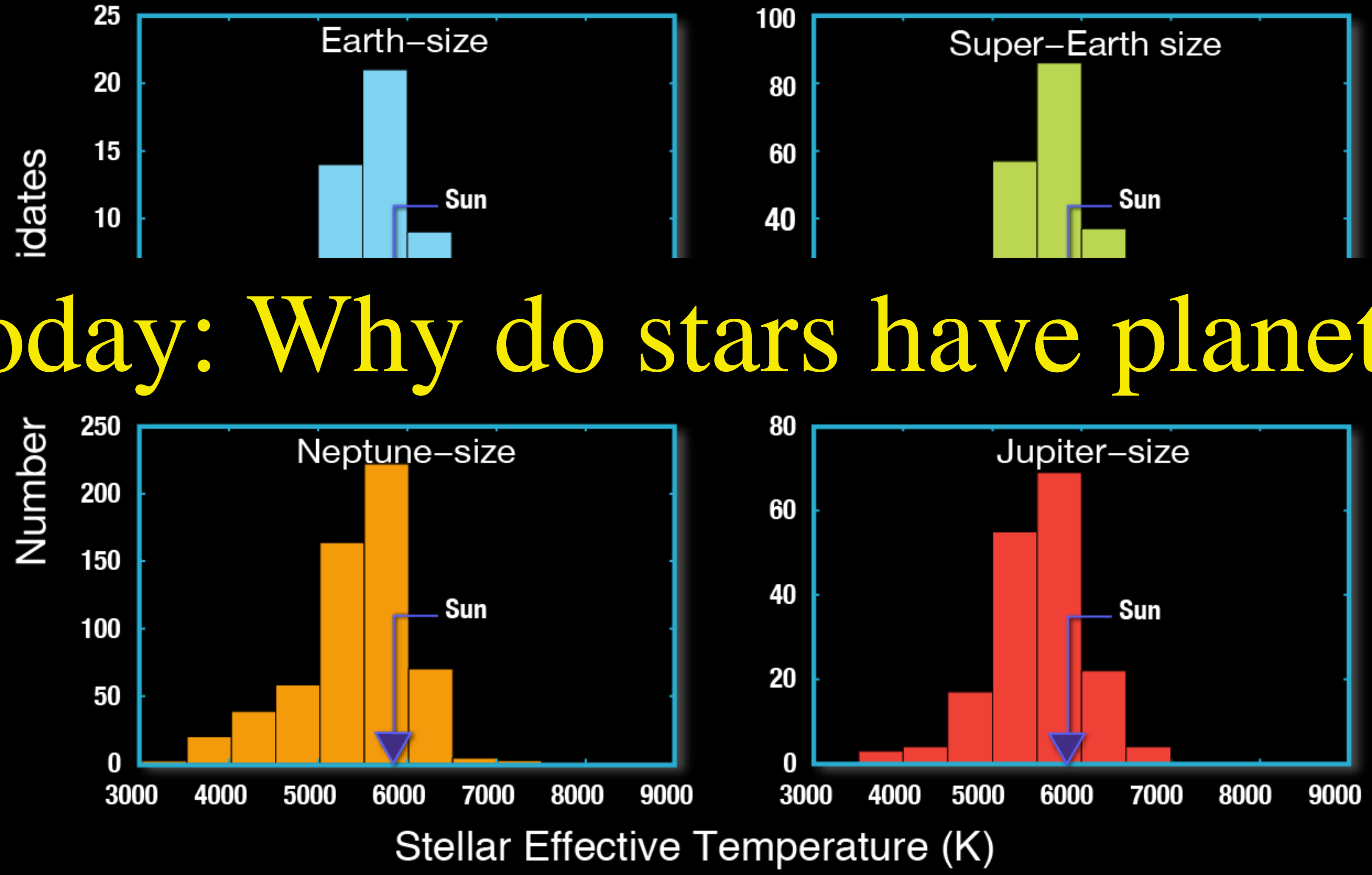

Today: Why do stars have planets?

Inside-out collapse model of Shu (1977)

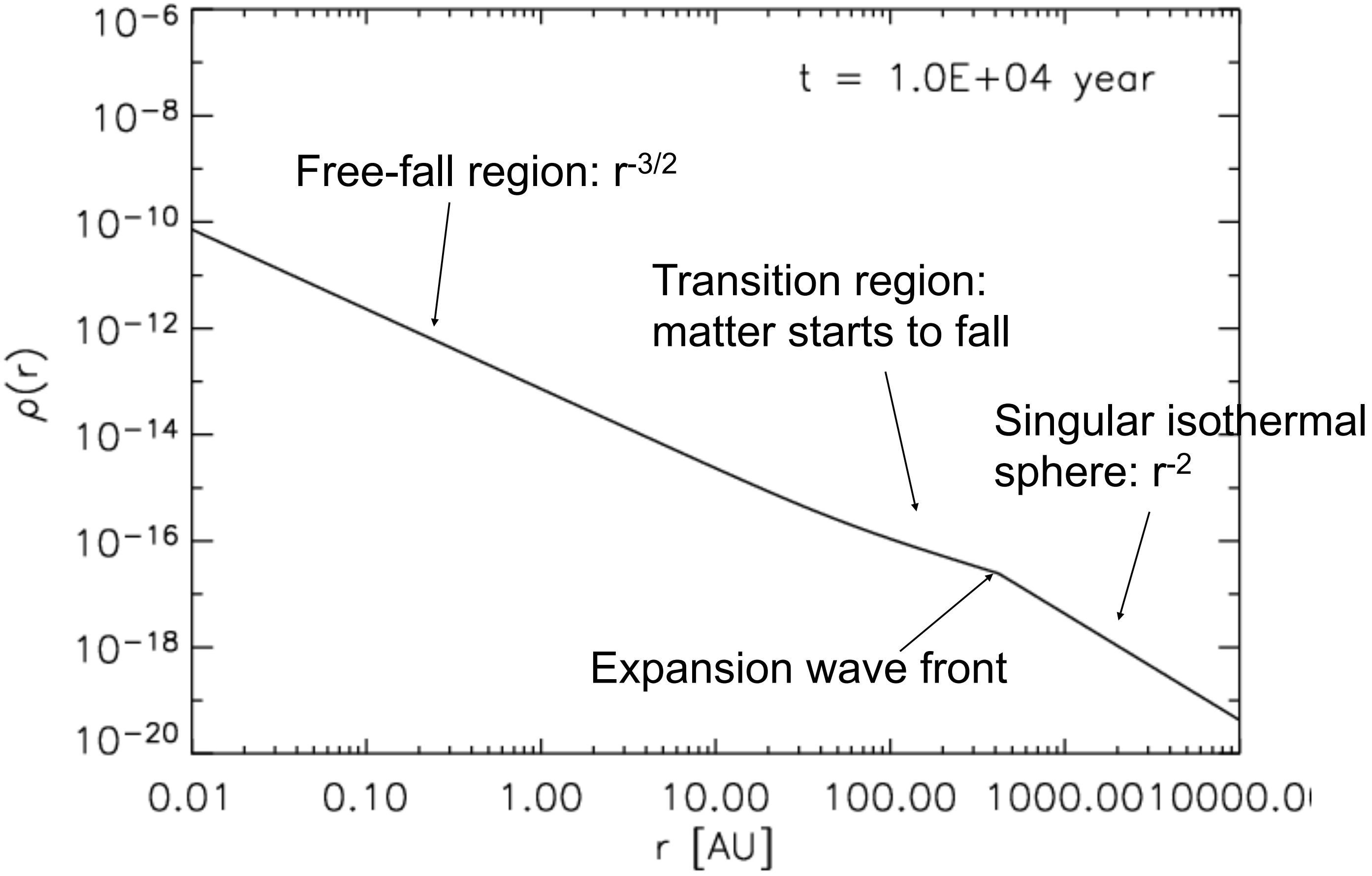

Free-fall region: $r^{-3/2}$

Transition region: matter starts to fall

Singular isothermal sphere: r^{-2}

Expansion wave front

Slide pirated from K. Dullemond

Inside-out collapse model of Shu (1977)

Deep down in free-fall region ($r << c_s t$):

$$\rho(r,t) = \frac{c_s^{3/2}}{17.96\,G}\frac{1}{\sqrt{t}}\frac{1}{r^{3/2}} \qquad v(r,t) = \sqrt{\frac{2GM_*(t)}{r}}$$

Accretion rate is constant: $$\dot{M} = \frac{c_s^3 m_0}{G} = 0.975\frac{c_s^3}{G}$$

Stellar mass grows linear in time

Slide pirated from K. Dullemond

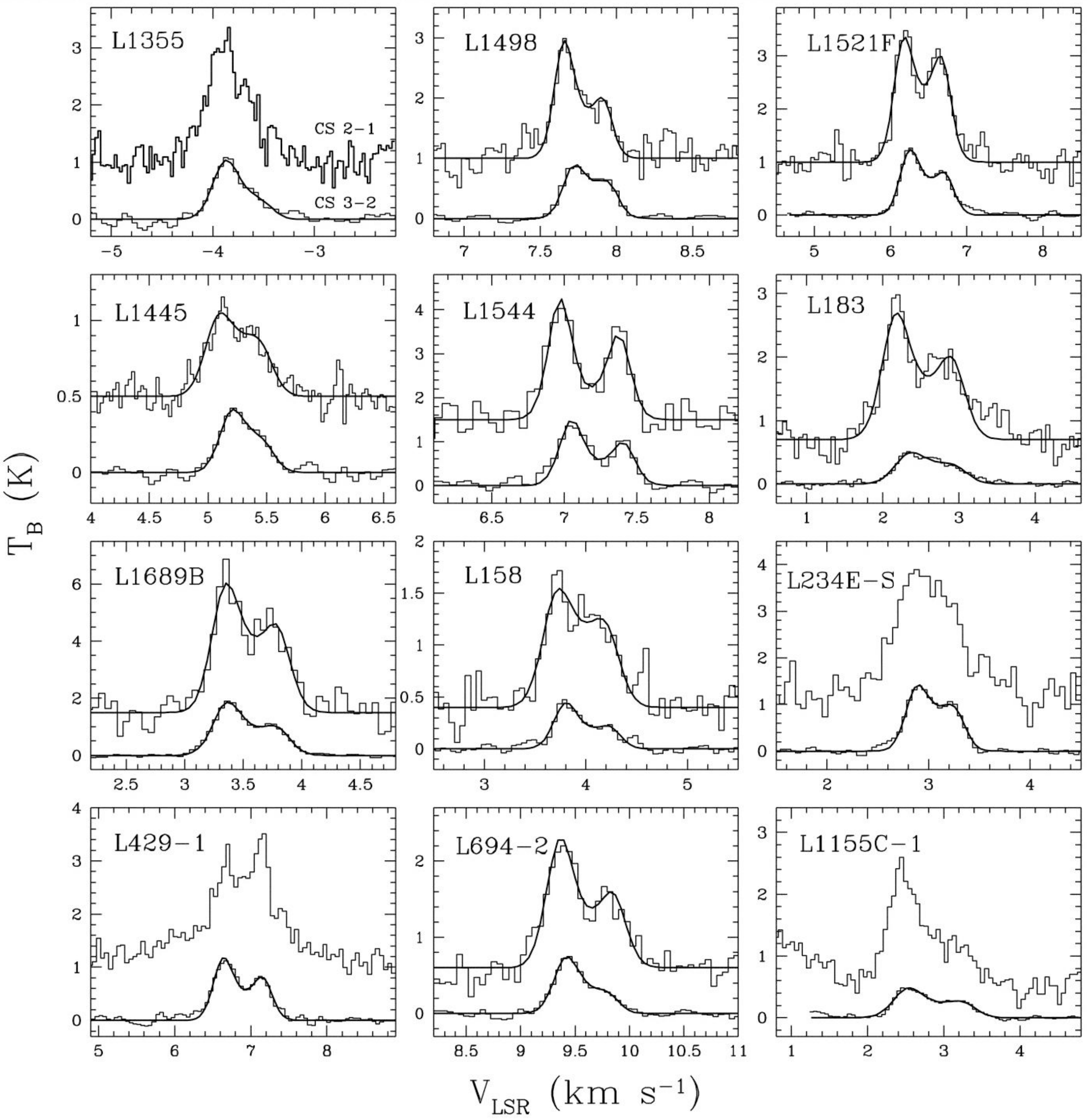

Infall in starless cores:

Lee, Myers & Plume
2004 ApJ 153, 523

Clear infall signature
for 18 of 94 starless

Inverse P-Cygni Profiles toward the Protostar IRAS 4A

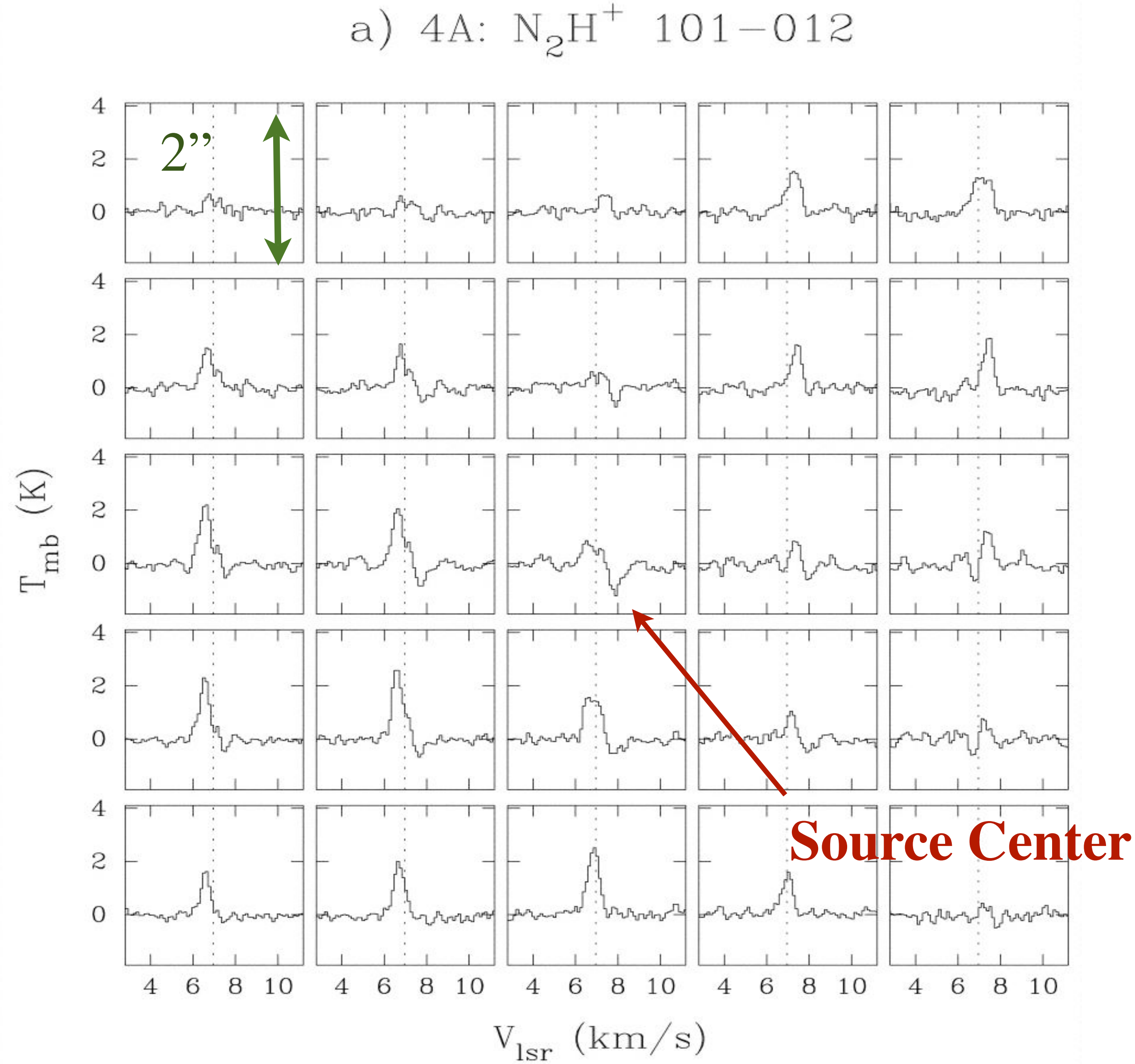

Infall velocities of ~ 0.5 km s^{-1}

DiFrancesco et al. ApJ 2001 562, 770

Problem 1: How can we detect protostars?

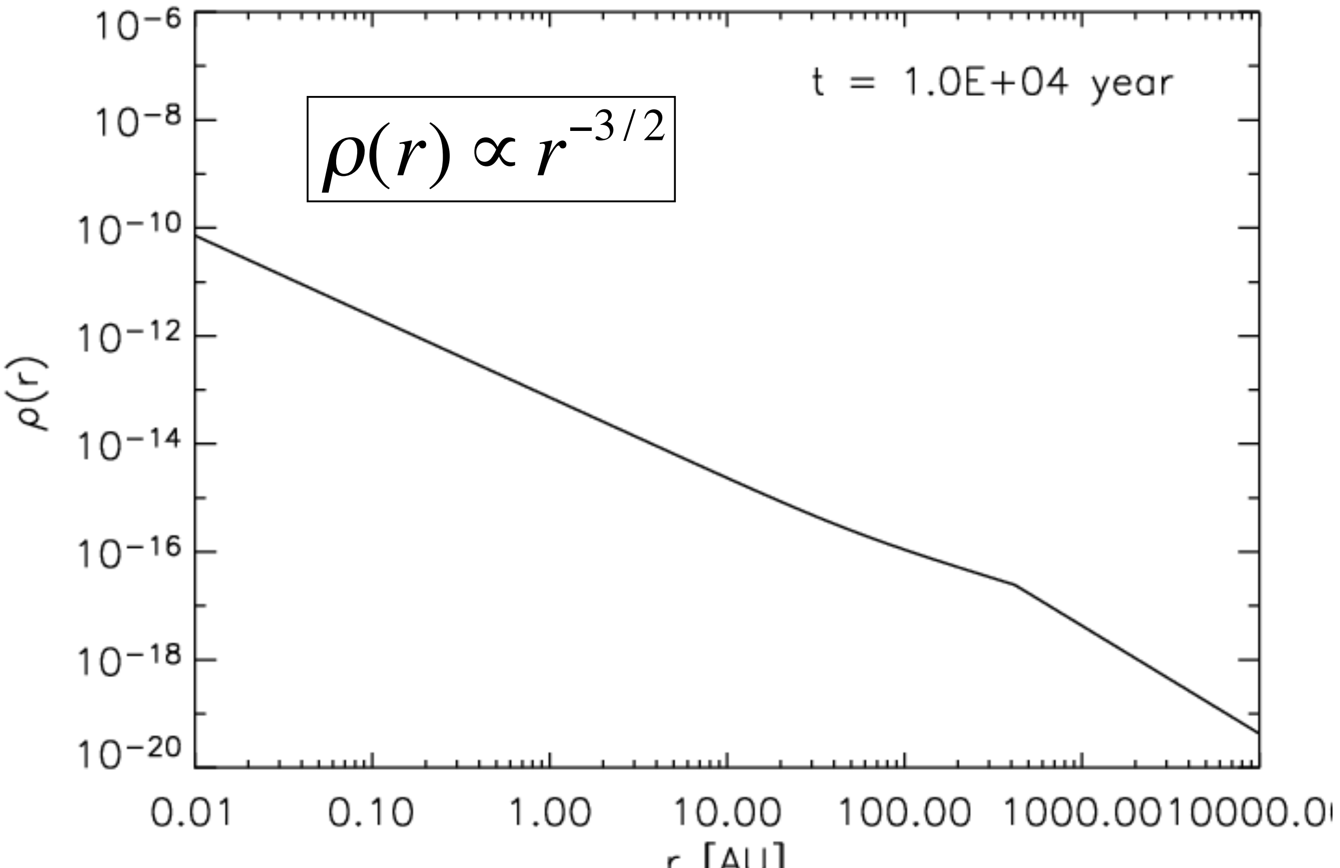

For a Spherical Core

Deep down in free-fall region ($r \ll c_s t$):

$$\rho(r,t) = \frac{c_s^{3/2}}{17.96G}\frac{1}{\sqrt{t}}\frac{1}{r^{3/2}}$$

$$v(r,t) = \sqrt{\frac{2GM_*(t)}{r}}$$

$$N(H_2) = \int_{r_{min}}^{\infty} \frac{1}{\mu m_H}\rho(r)dr$$

$$N(H_2) = \int_{r_{min}}^{\infty} \frac{\rho(r_0)}{\mu m_H}\left(\frac{r_0}{r}\right)^{3/2} dr$$

$$N(H_2) = \frac{2\rho(r_0)r_0}{\mu m_H}\left(\frac{r_0}{r_{min}}\right)^{1/2}$$

for r_{inner} = 1 AU &
r_{outer} = 10,000 AU
t = 100,000 year
c_s = .24 km s^{-1} (t = 20 K)

=> A_V = 300

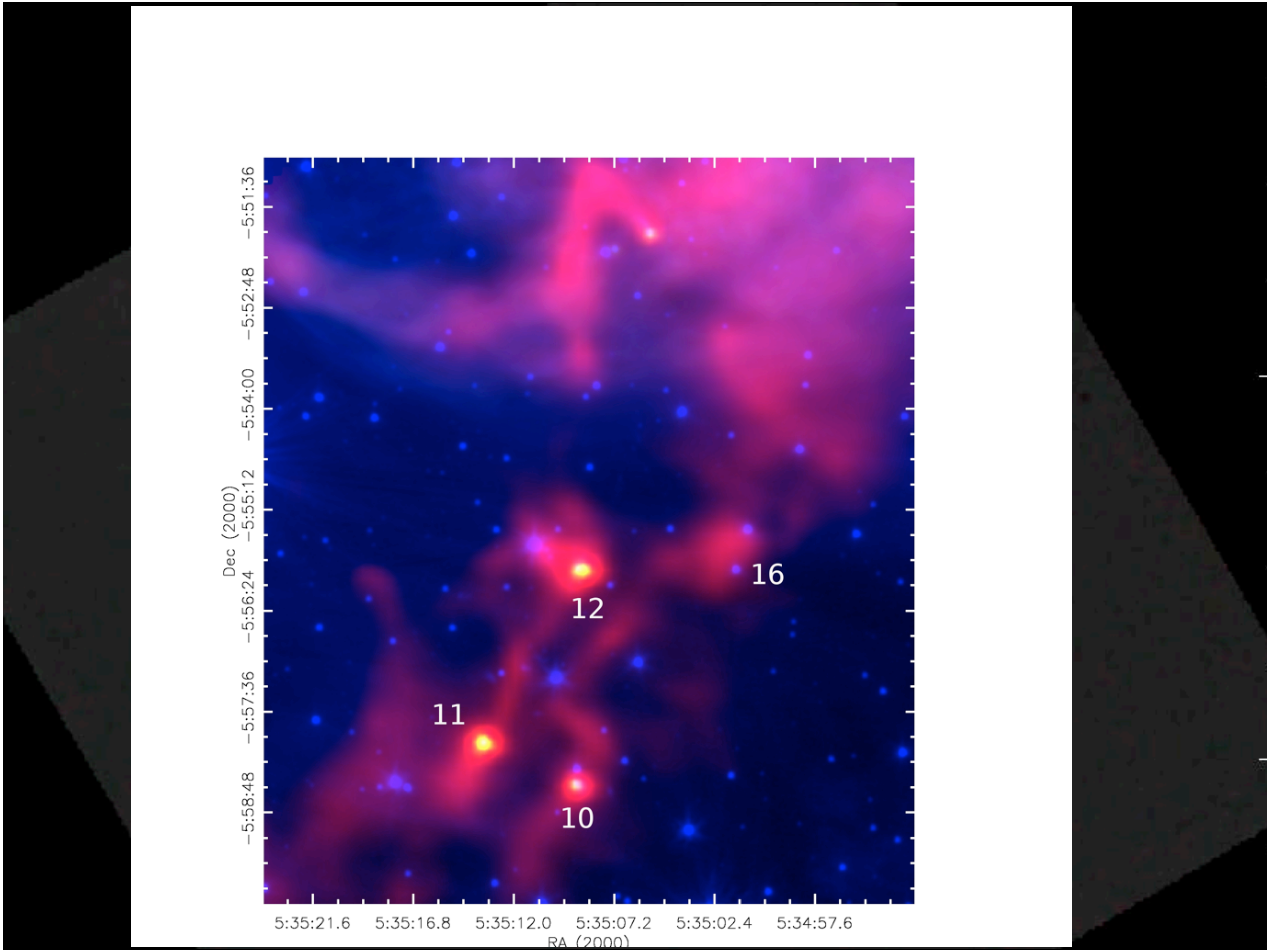
−5:51:36
−5:52:48
−5:54:00
−5:55:12
−5:56:24
−5:57:36
−5:58:48
Dec (2000)
5:35:21.6
5:35:16.8
5:35:12.0
5:35:07.2
5:35:02.4
5:34:57.6
RA (2000)
16
12
11
10

Problem Number 2: Why do stars rotate so slowly?

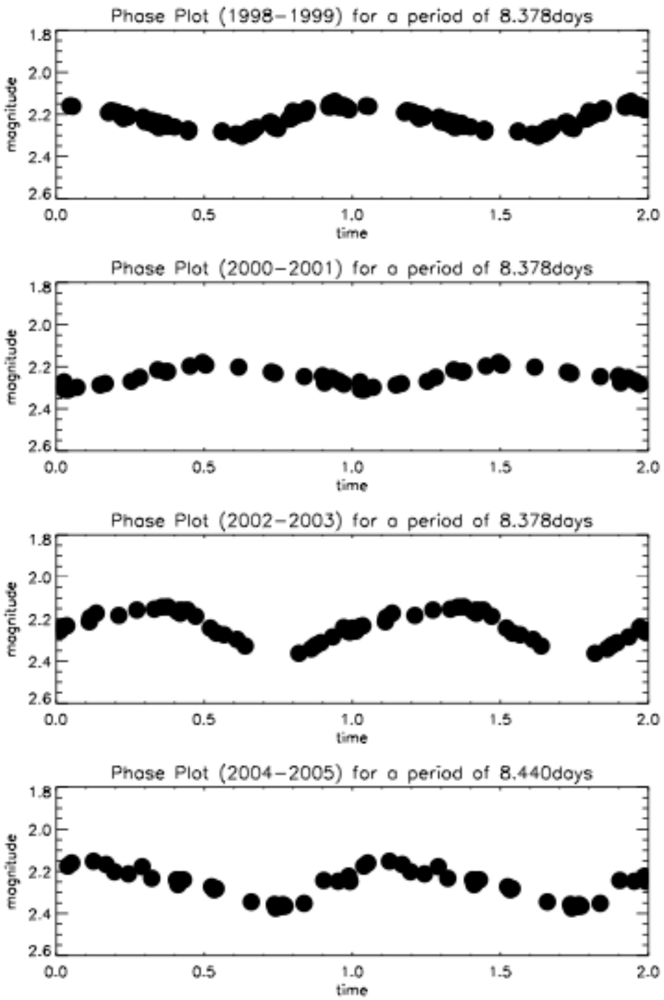

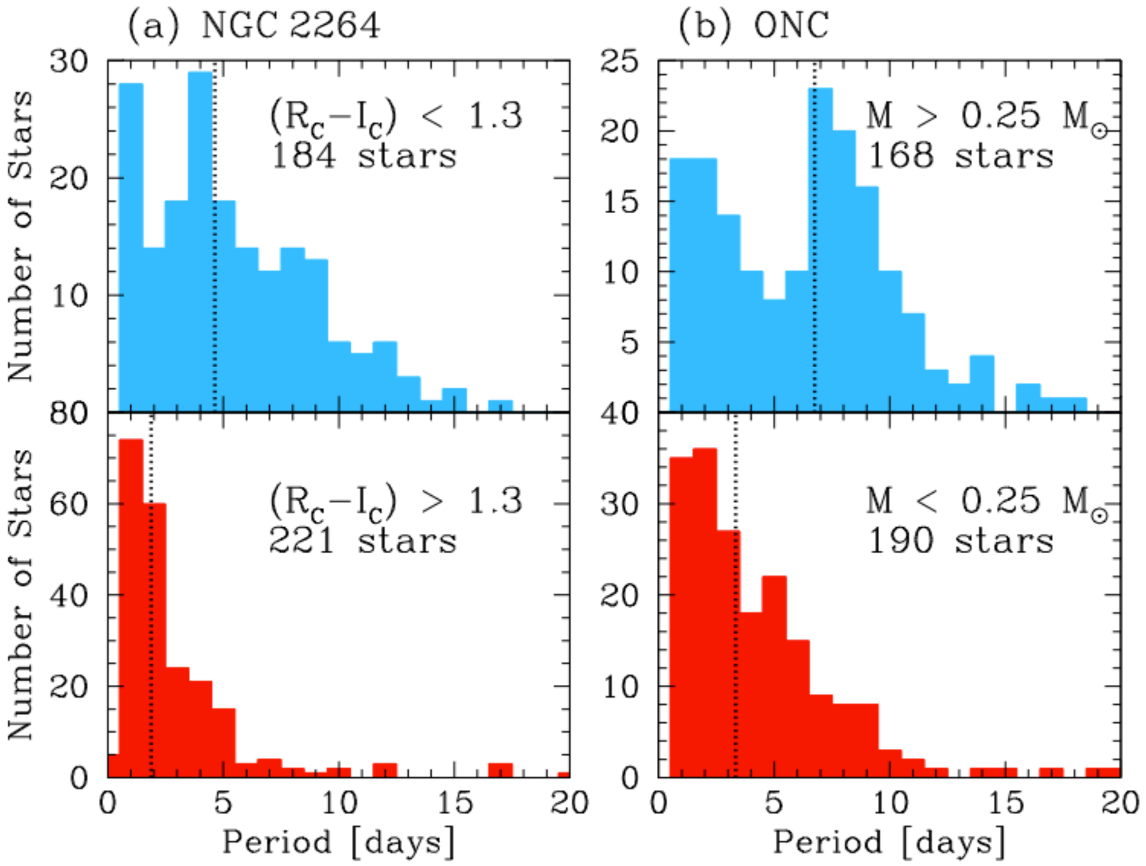

Herbst: http://arxiv.org/abs/astro-ph/0603673

Core Rotation

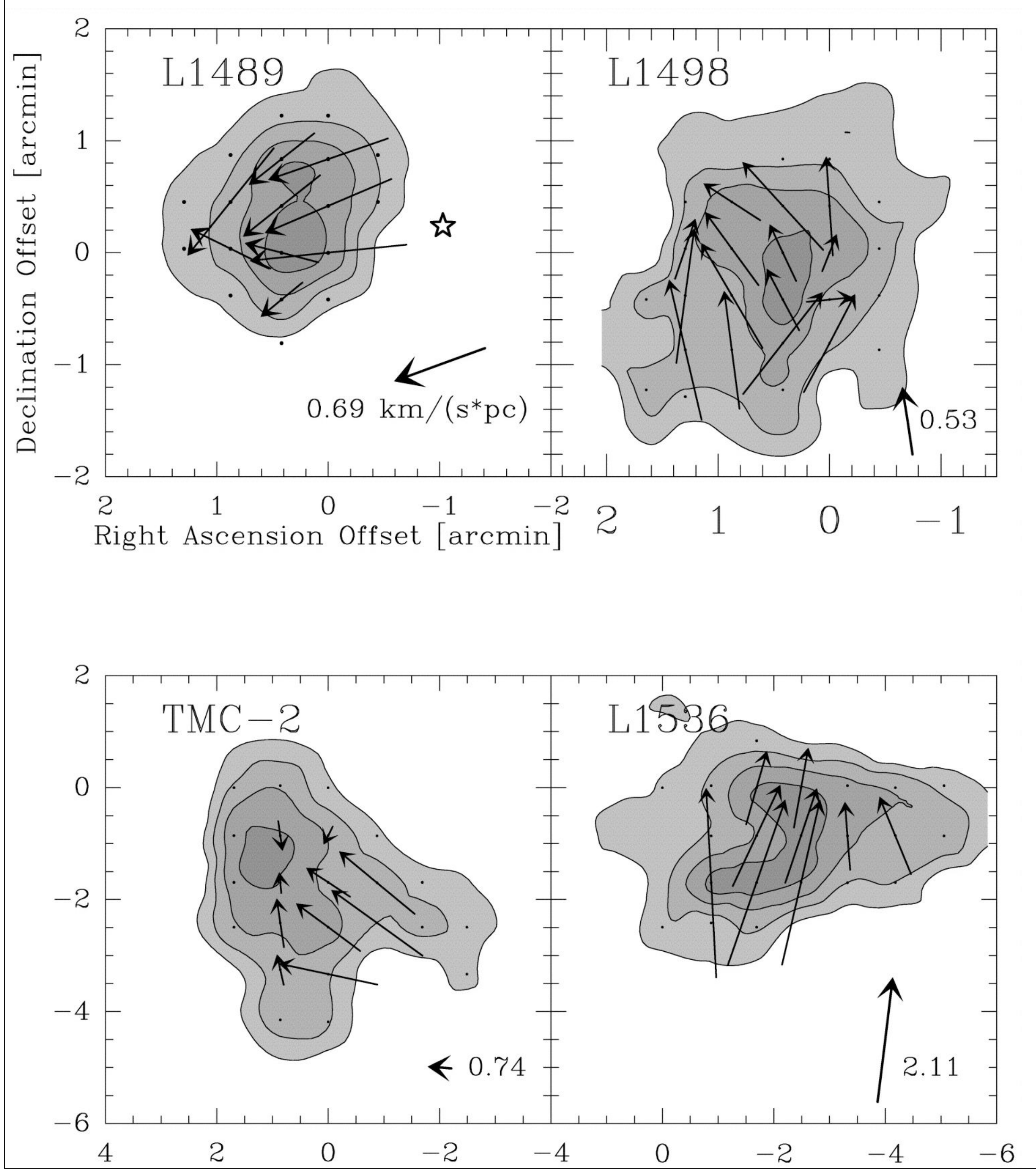

Caselli et al. 2002
ApJ 572, 238

N_2H^+ maps of dense cores

Gradients:

0.5-6 km s^{-1} pc^{-1}

Rotation kinetic energy/gravitational energy = 10^{-4} to 0.07

Conservation of Angular Momentum

$L/M = V\ R\ = (\Delta V/\Delta R)\ R^2$ where $(\Delta V/\Delta R)$ is the gradient in velocity per pc

$L/M = 0.5 \times 10^5$ cm s^{-1}/pc x $(0.05\ \mathrm{pc})^2$ x 3×10^{18} cm/pc

$L/M = 3.8 \times 10^{21}\ \mathrm{cm}^2\ \mathrm{s}^{-1}$

When radius shrinks from 0.05 pc to 7×10^{10} cm

$L/M = 2\ \pi\ \Omega\ R^2$

$R = 7 \times 10^{10}$ cm $\Rightarrow \Omega < 1$ sec

Stars should be rotating much faster

We have left a major component of collapse out: Rotation

Collapse of rotating clouds

Solid-body rotation of cloud:

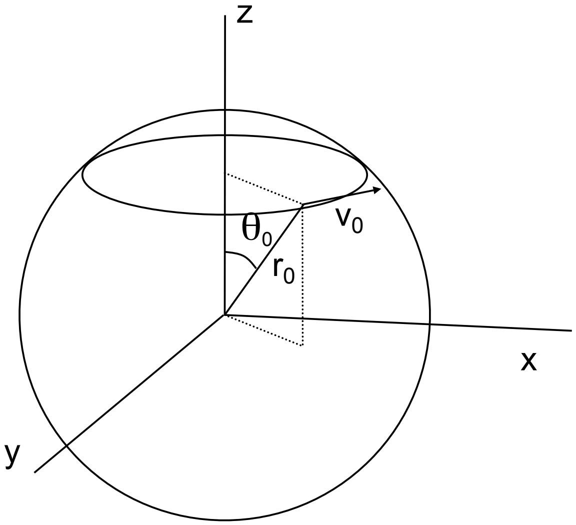

$$v_0 = \omega\, r_0 \sin\theta_0$$

$$j = r_0 v_0 << \sqrt{GM\, r_0}$$

Infalling gas-parcel falls *almost* radially inward, but close to the star, its angular momentum starts to affect the motion.

At that radius $r<<r_0$ the kinetic energy $v^2/2$ vastly exceeds the initial kinetic energy. So one can say that the parcel started almost without energy.

Slide pirated from K. Dullemond

Collapse of rotating clouds

Focal point of ellipse/parabola: $a + r = \mathrm{const} \;\; = \mathrm{r_e} \;\; = 2\mathrm{r_m}$

No energy condition: $e_{\mathrm{tot}} \equiv \frac{v^2}{2} - \frac{GM}{r} \cong 0$ $\boxed{v_{\mathrm{m}}^2 = \frac{2GM}{r_{\mathrm{m}}}}$

Ang. Mom. Conserv: $j^2 = v_{\mathrm{m}}^2 r_{\mathrm{m}}^2 = 2GM\, r_{\mathrm{m}} = GM\, r_{\mathrm{e}}$

Radius at which parcel hits the equatorial plane:

$$\boxed{r_{\mathrm{e}} = \frac{j^2}{GM} = \frac{\omega^2 r_0^4 \sin^2\theta_0}{GM}}$$

$$v_0 = \omega\, r_0 \sin\theta_0$$

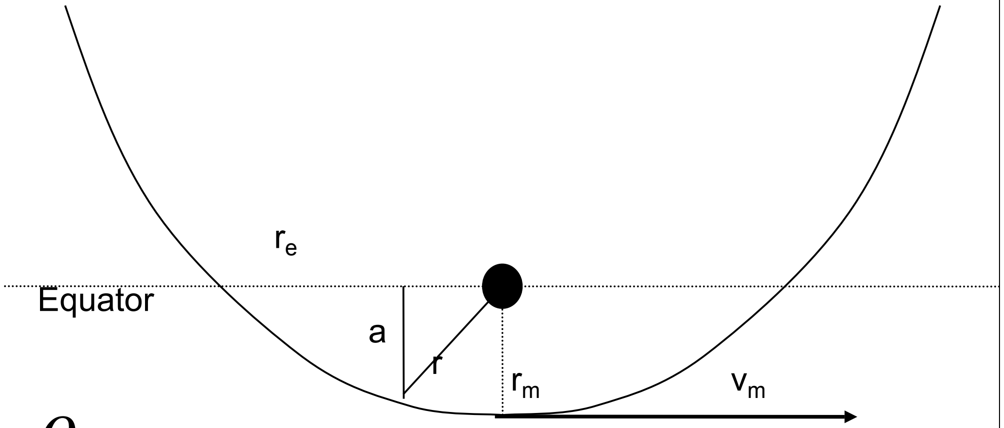

Slide pirated from K. Dullemond

Collapse of rotating clouds

For larger θ_0: larger r_e

For given shell (i.e. given r_0), all the matter falls within the centrifugal radius r_c onto the midplane.

$$r_c = r_e(\theta_0 = \pi/2) = \frac{\omega^2 r_0^4}{GM}$$

If $r_c < r_*$, then mass is loaded directly onto the star

If $r_c > r_*$, then a disk is formed

In Shu model, $r_0 \sim t$, and therefore:

$$\boxed{r_c \propto t^4}$$

Slide pirated from K. Dullemond

Angular Momentum leads to Disk

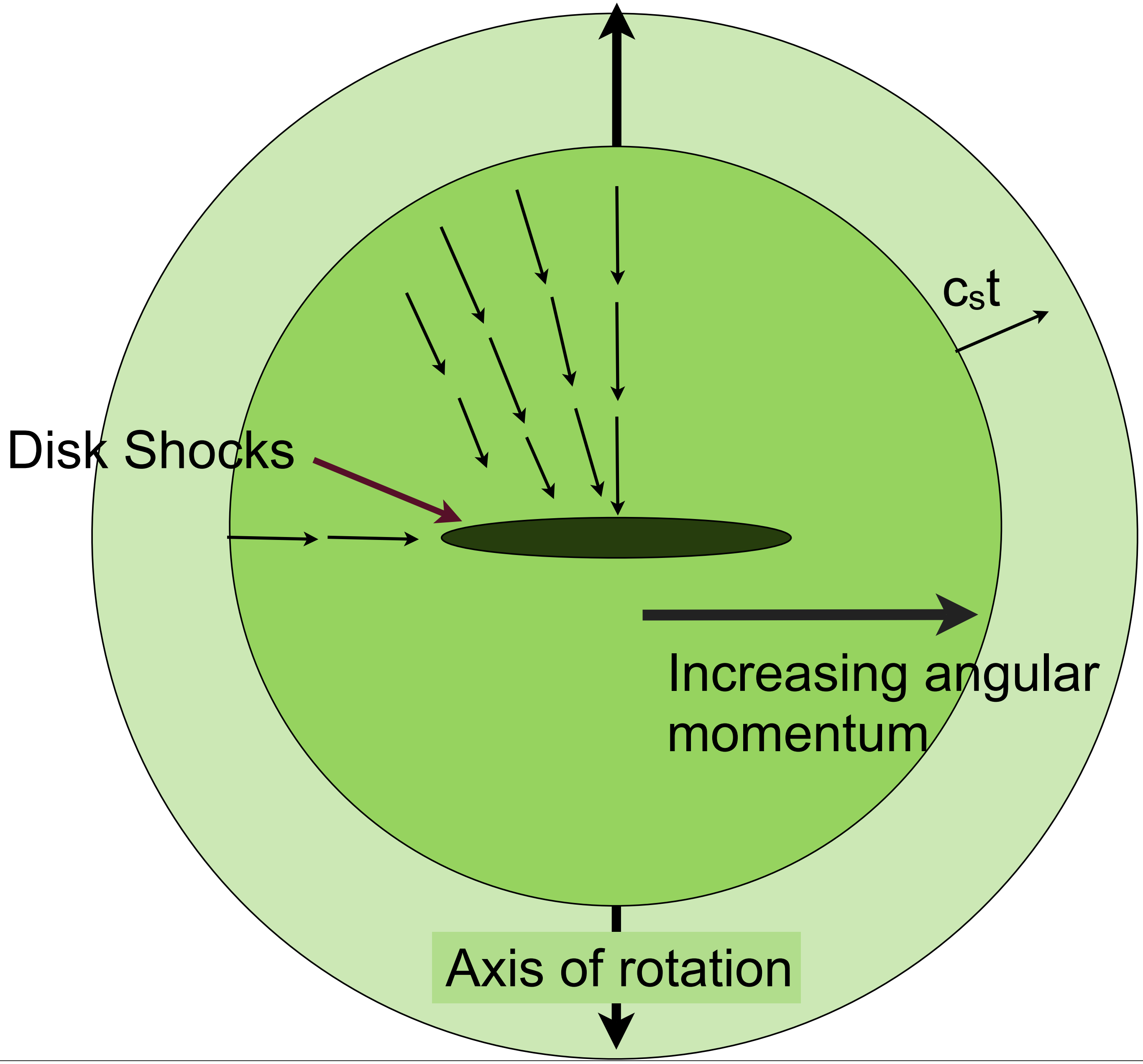

Collapse of Rotating Core

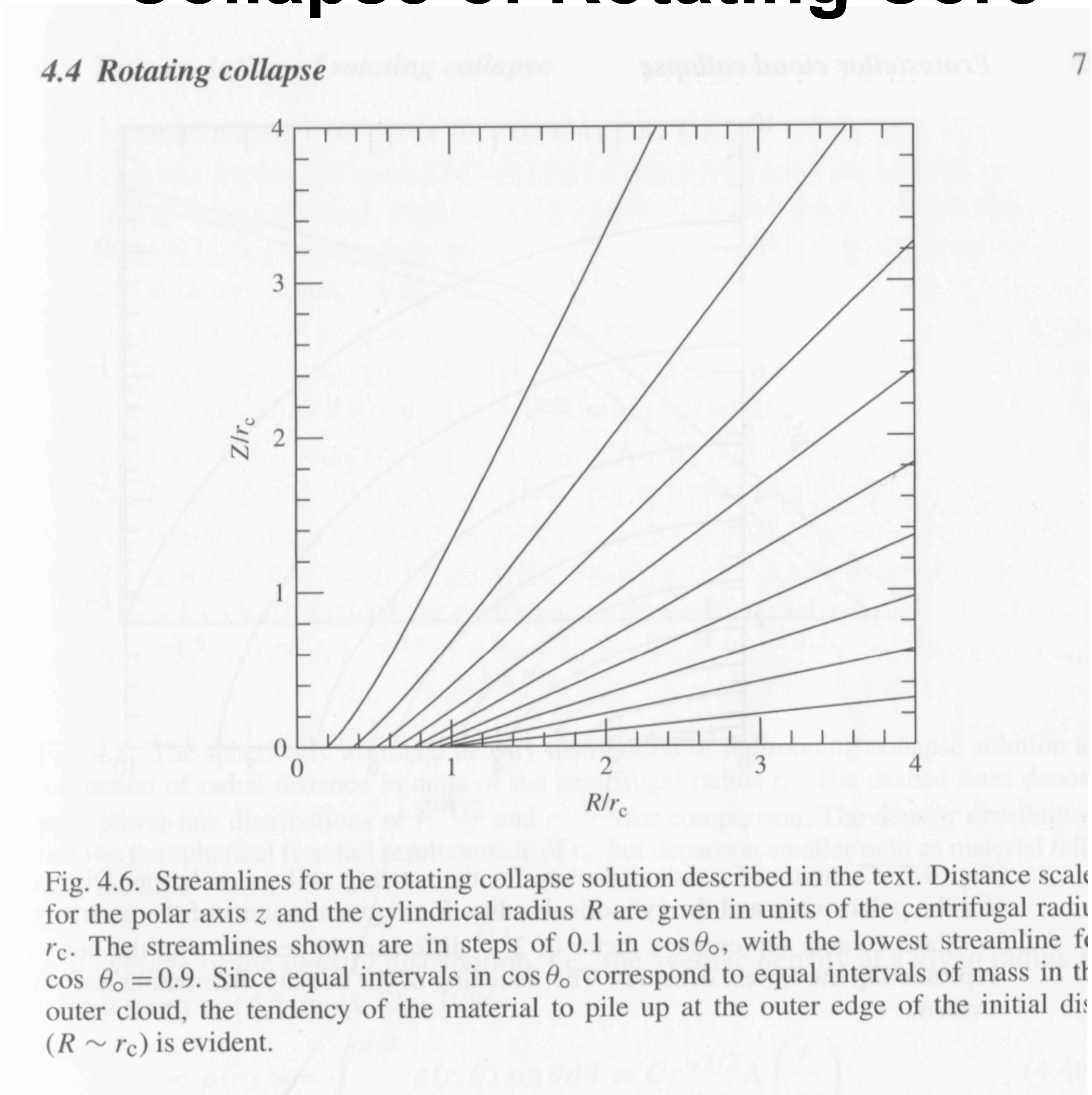

Fig. 4.6. Streamlines for the rotating collapse solution described in the text. Distance scal for the polar axis z and the cylindrical radius R are given in units of the centrifugal radiu r_c. The streamlines shown are in steps of 0.1 in $\cos\theta_\circ$, with the lowest streamline f $\cos\ \theta_\circ = 0.9$. Since equal intervals in $\cos\theta_\circ$ correspond to equal intervals of mass in th outer cloud, the tendency of the material to pile up at the outer edge of the initial di ($R \sim r_c$) is evident.

Collapse of Rotating Core

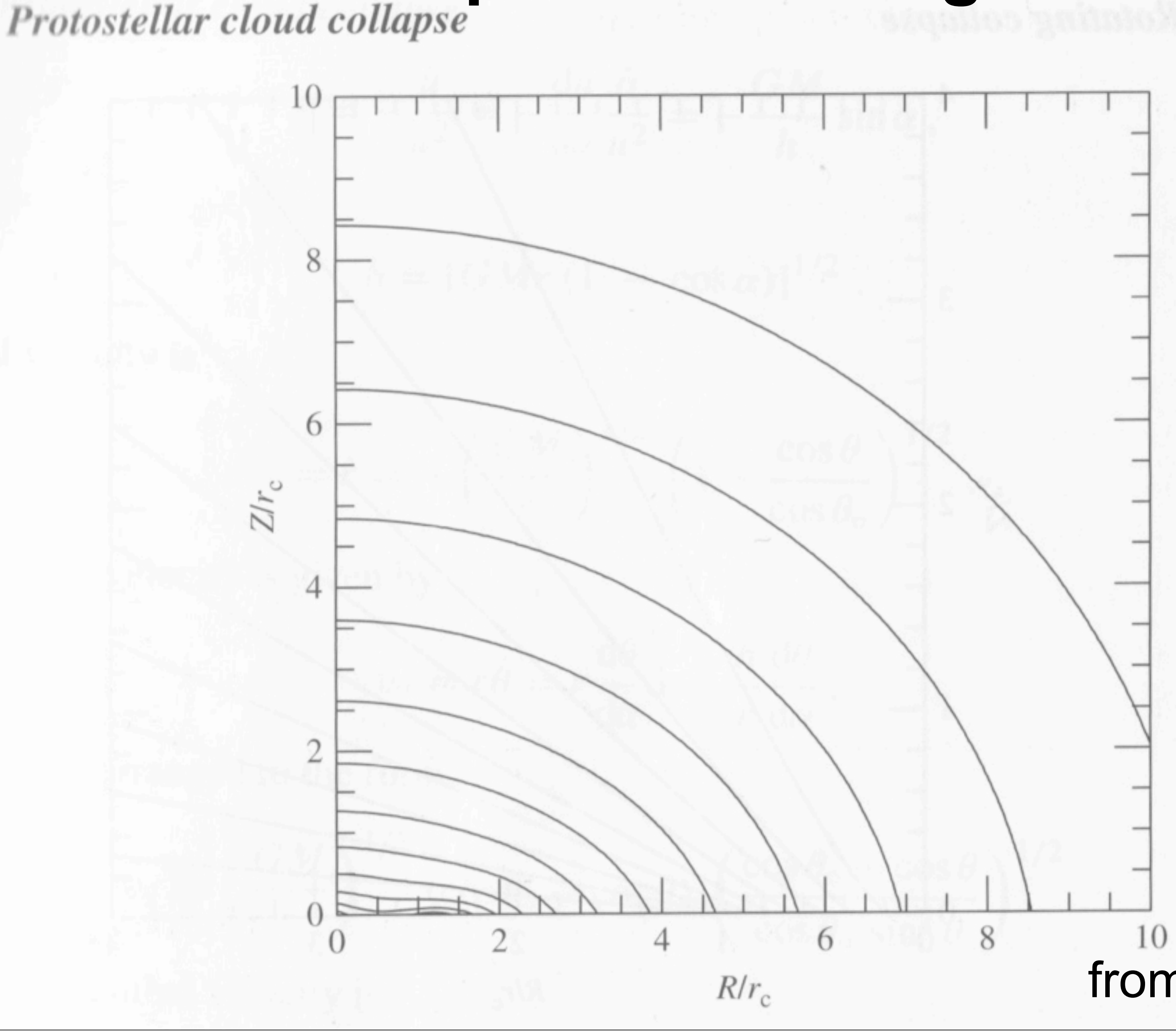

from Hartmann

Collapse of Rotating Core

from Hartmann

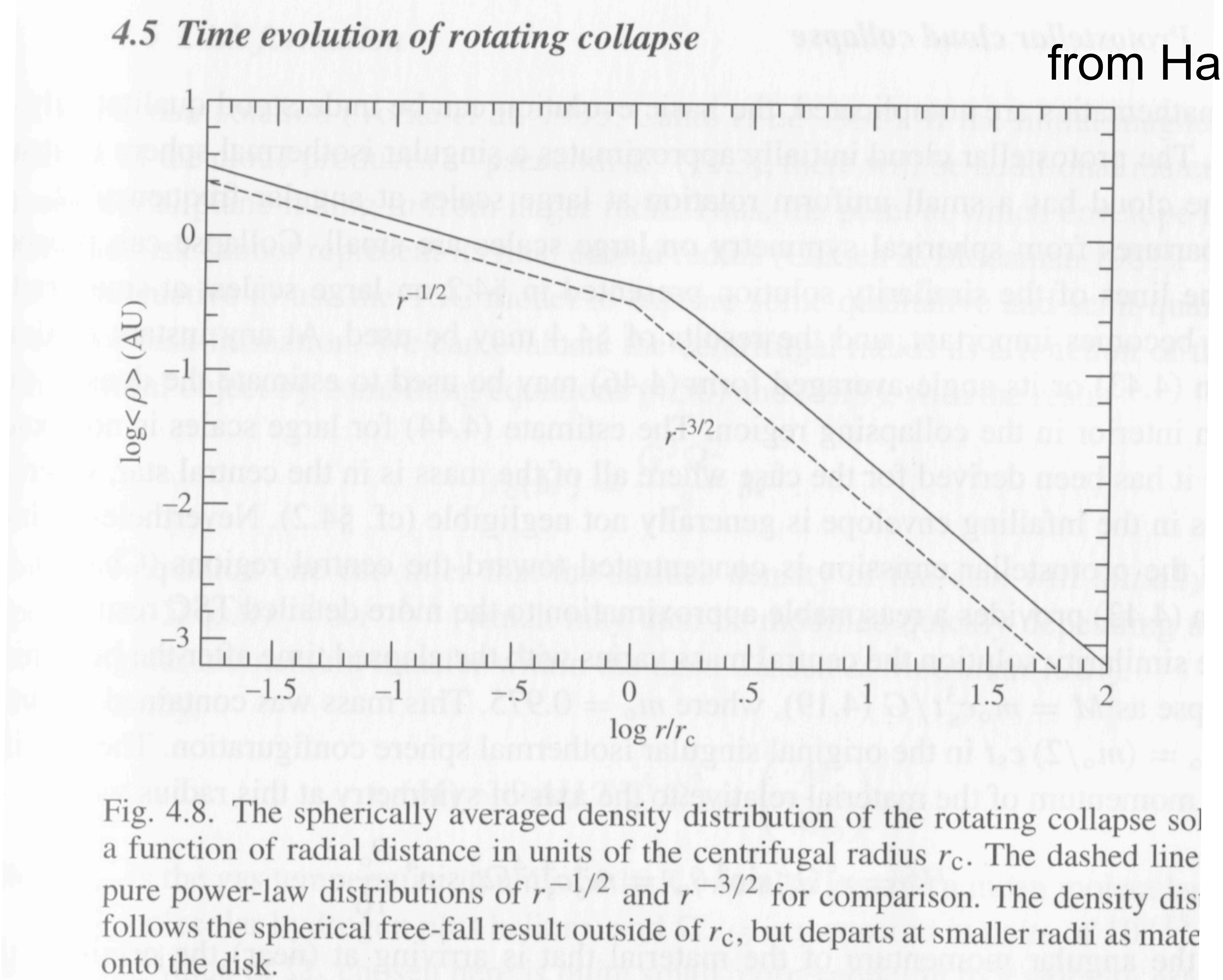

4.5 Time evolution of rotating collapse

Fig. 4.8. The spherically averaged density distribution of the rotating collapse sol a function of radial distance in units of the centrifugal radius r_c. The dashed line pure power-law distributions of $r^{-1/2}$ and $r^{-3/2}$ for comparison. The density dis follows the spherical free-fall result outside of r_c, but departs at smaller radii as mate onto the disk.

from Hartmann

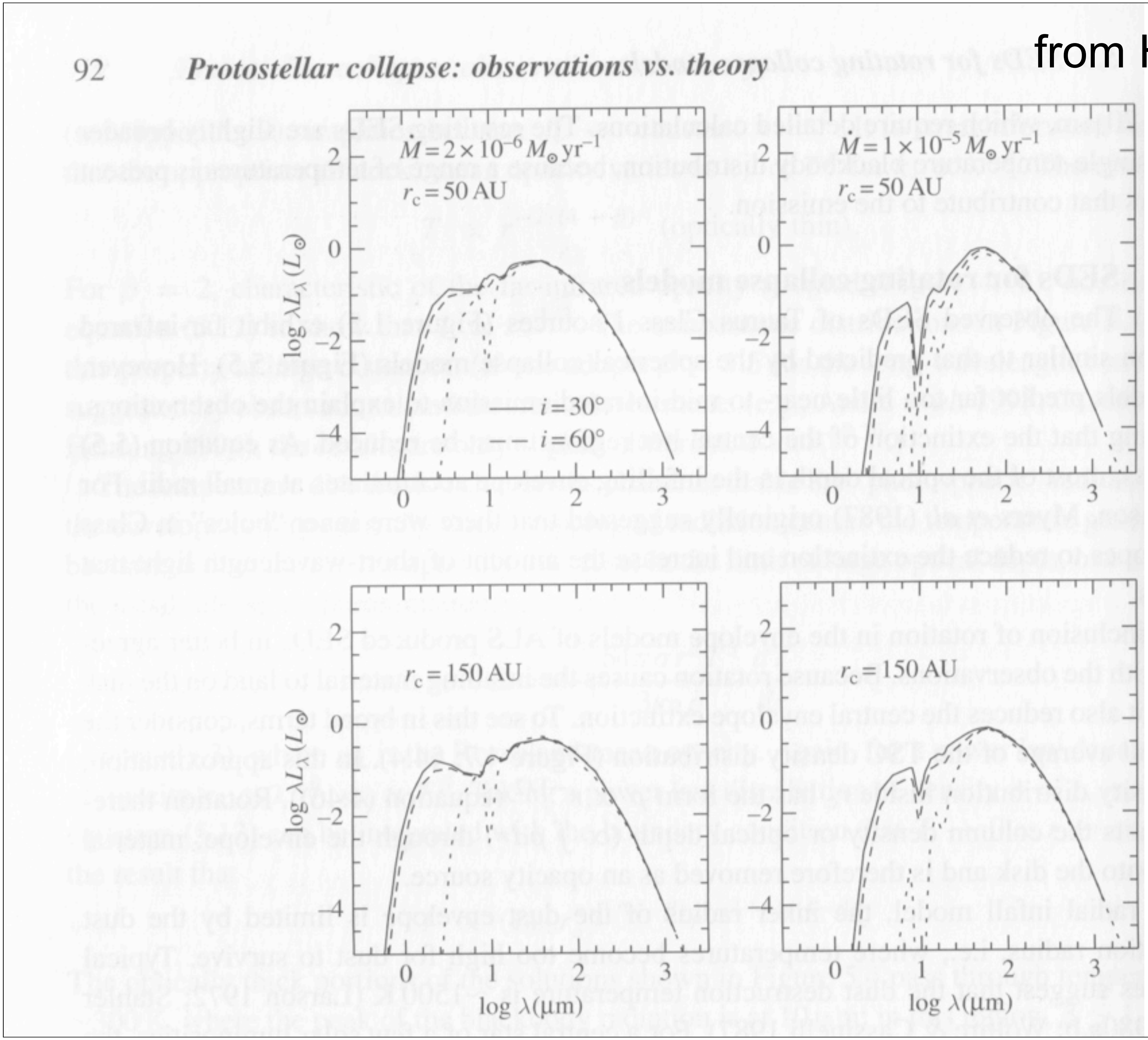

92 *Protostellar collapse: observations vs. theory*

Fitting Protostars with Rotating Collapse

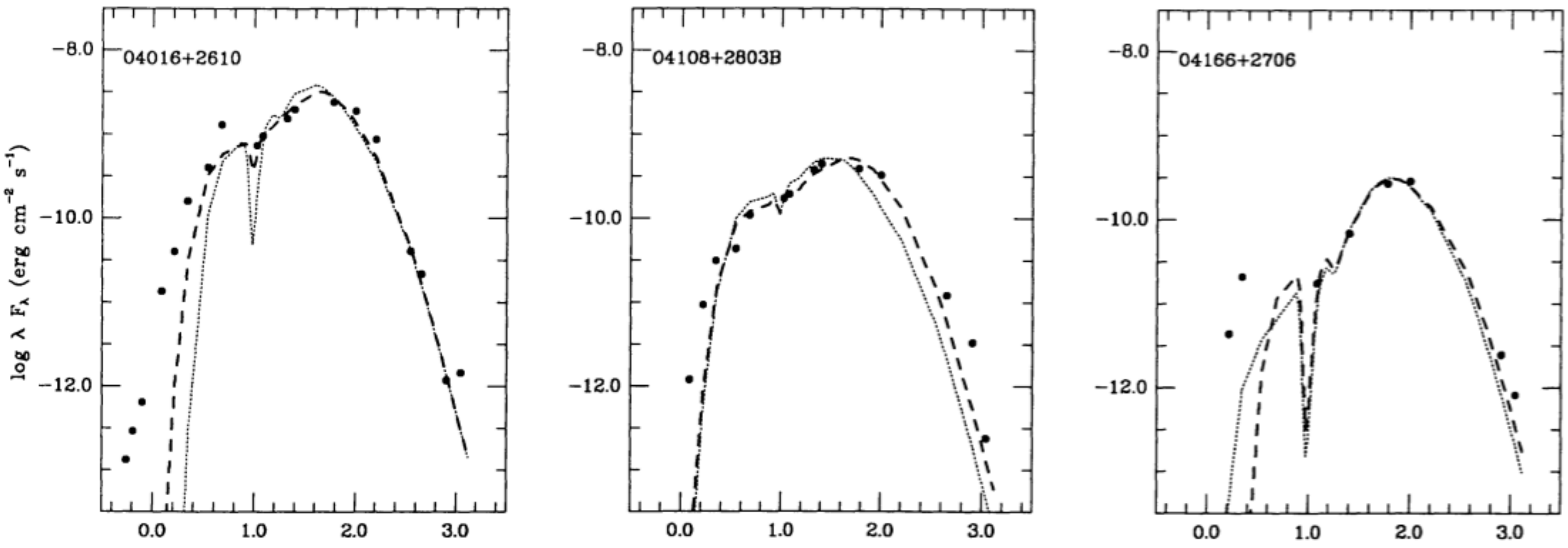

Kenyon, Calvet & Hartmann 1993

Angular Momentum Solved?

- Most of the angular momentum is in the disk!
- Most of the angular momentum of planetary systems in the planets!
- Still, how does the gas get from the rotating disk to the star?

Other means for getting rid of angular momentum:

Magnetic braking (magnetic field lines connect rotating core with surrounding cloud, and can transfer angular momentum from core to cloud if core is rotating faster than cloud)

Binary formation

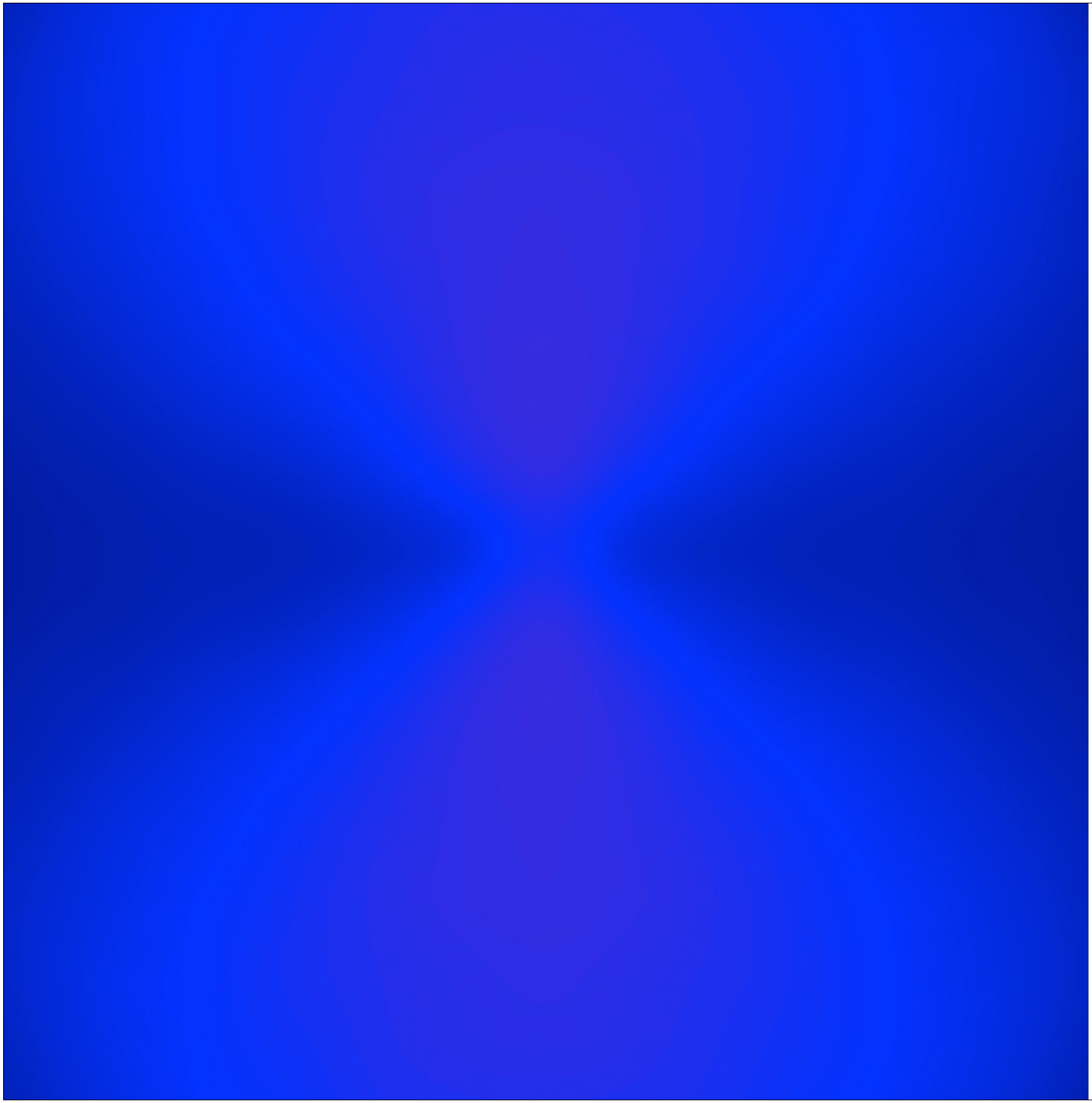

Bate 2000

Portrait of a Protostar

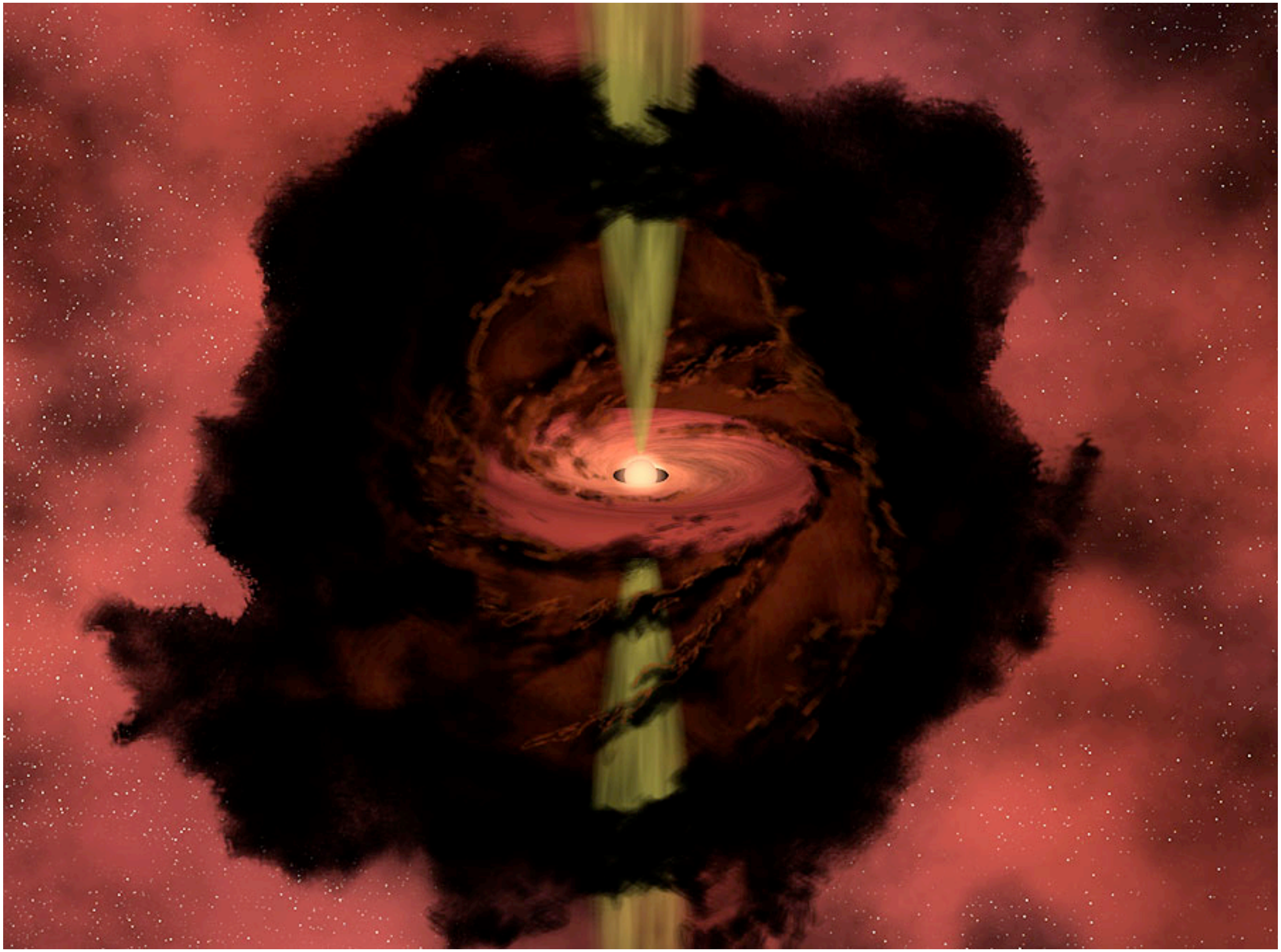

How does the gas get from the rotating disk to the star?

Protostellar disks and jets

- Most of infalling matter falls on the equator and forms a disk
- Friction within the disk causes matter to accrete onto the star
- Jets are often launched from the inner regions of these disks
- A jet penetrates through the infalling cloud and opens a cavity

Spectra of collapsing cloud + star + disk

Whitney et al. 2003

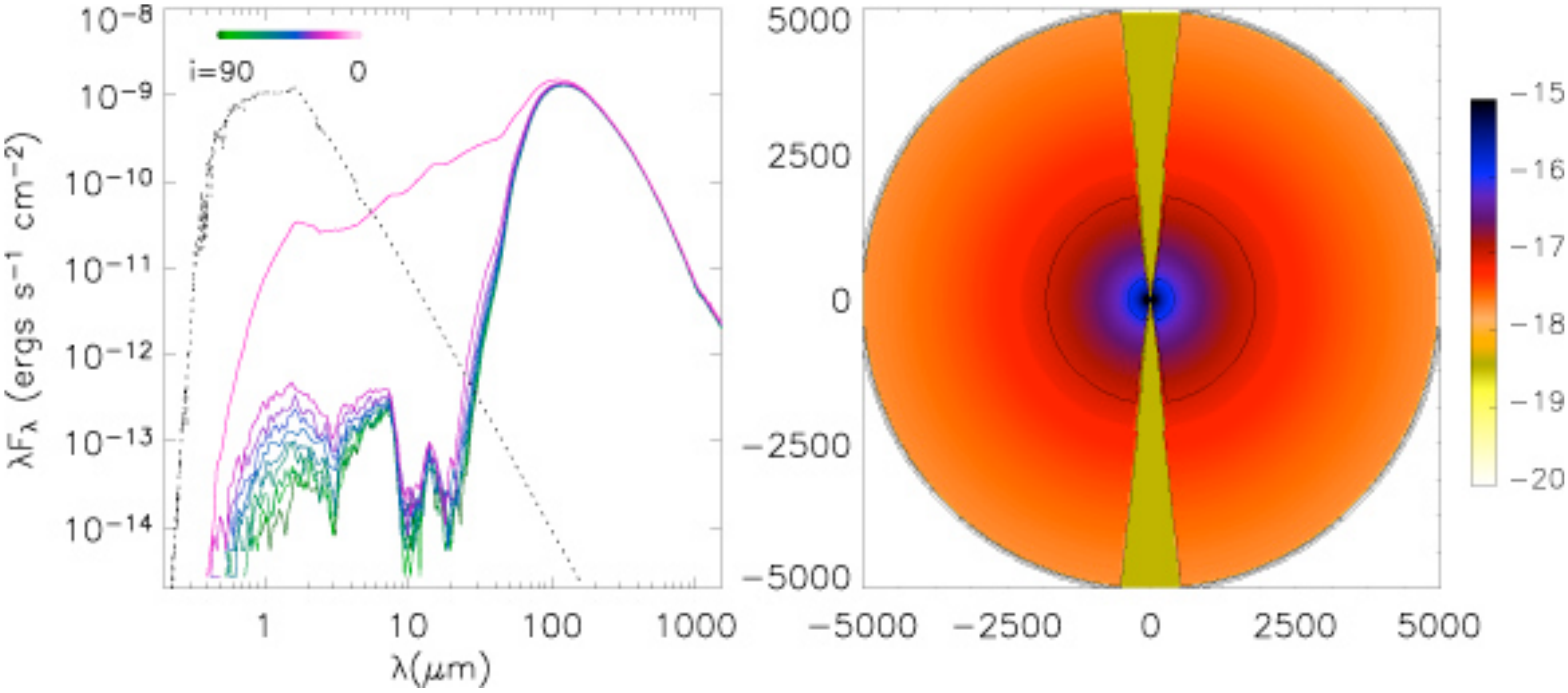

Class 0

Spectra of collapsing cloud + star + disk

Whitney et al. 2003

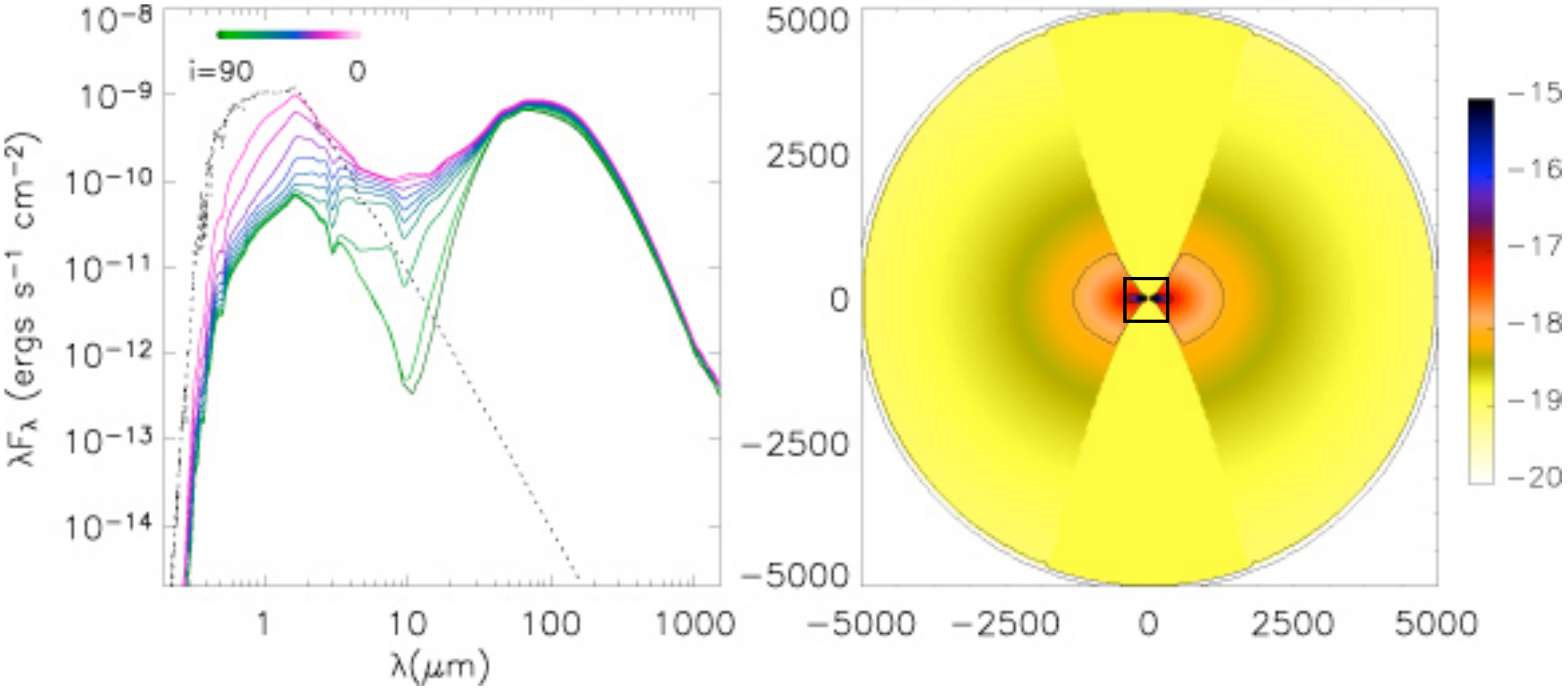

Class I

Spectra of collapsing cloud + star + disk

Whitney et al. 2003

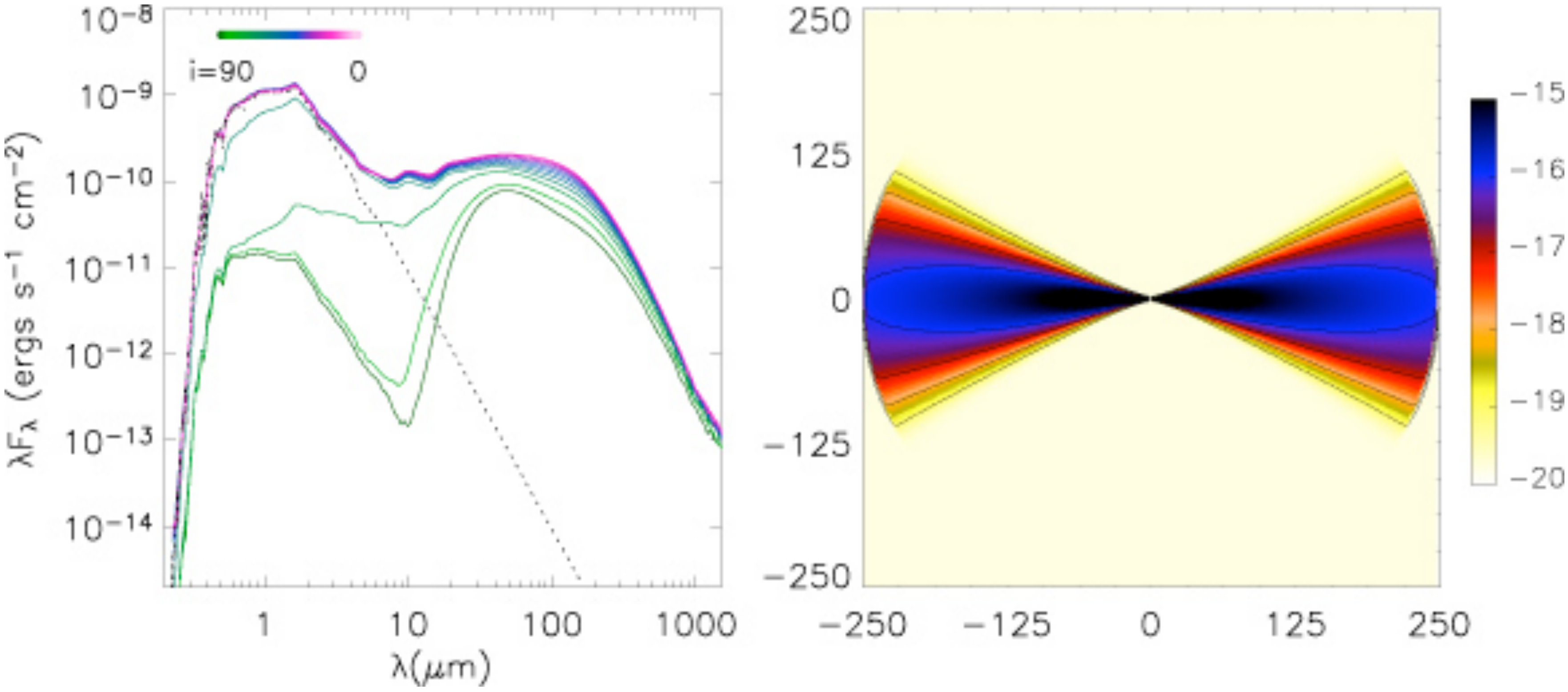

Class II

Spectra of collapsing cloud + star + disk

Whitney et al. 2003

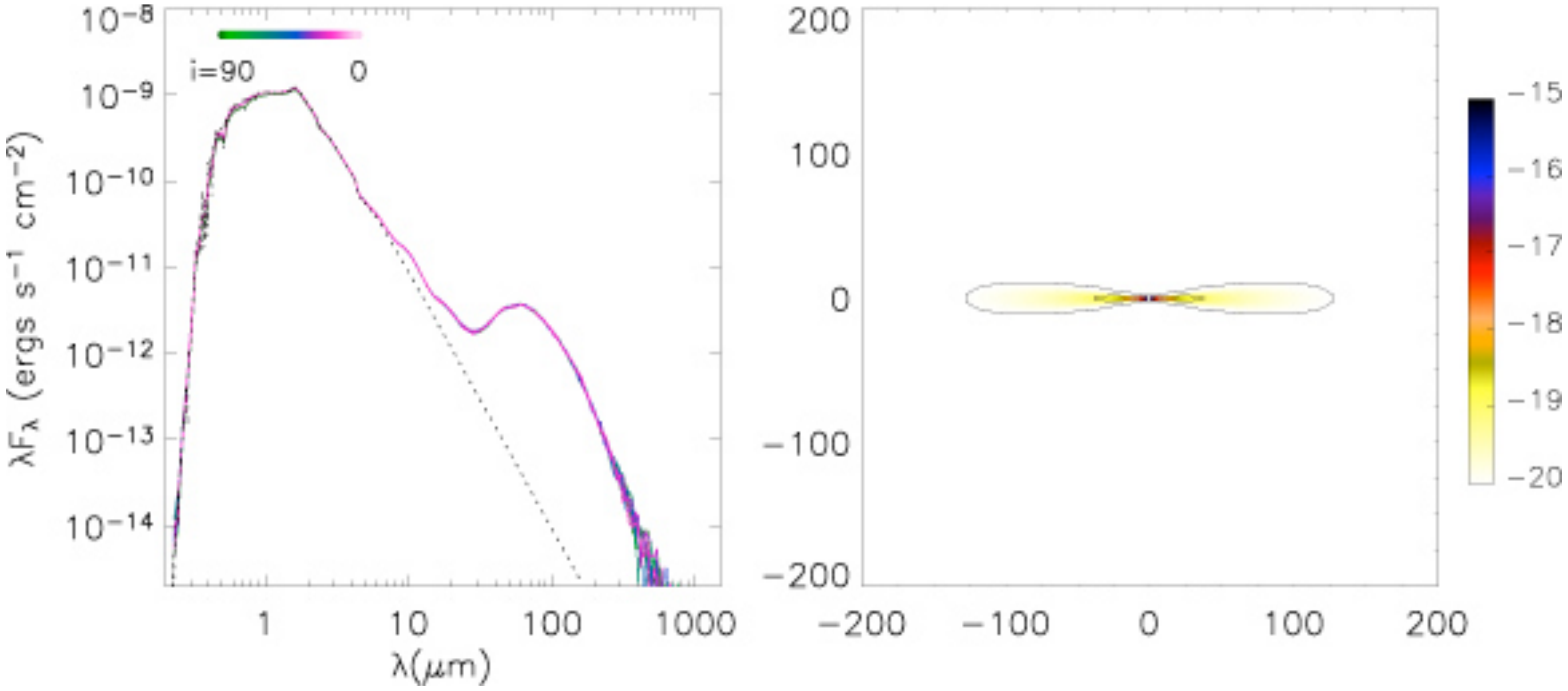

Class III

HOPS 136: A Case Study of an Edge-on Protostar

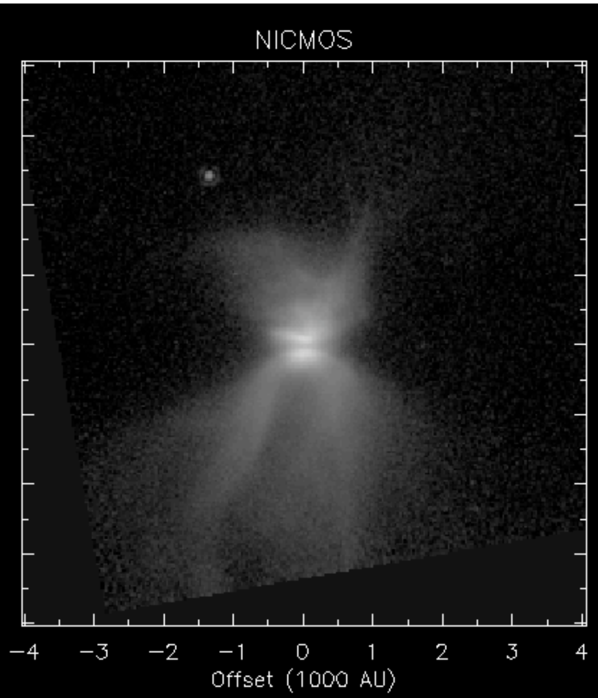

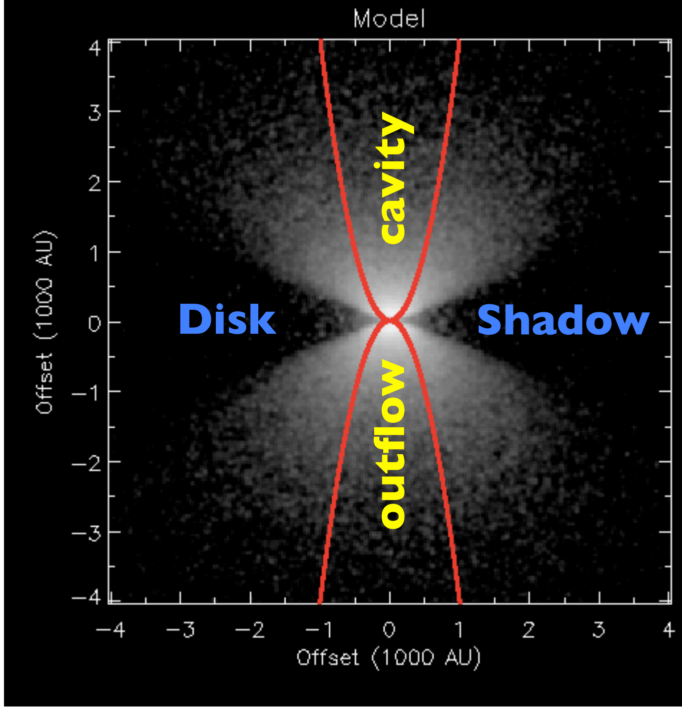

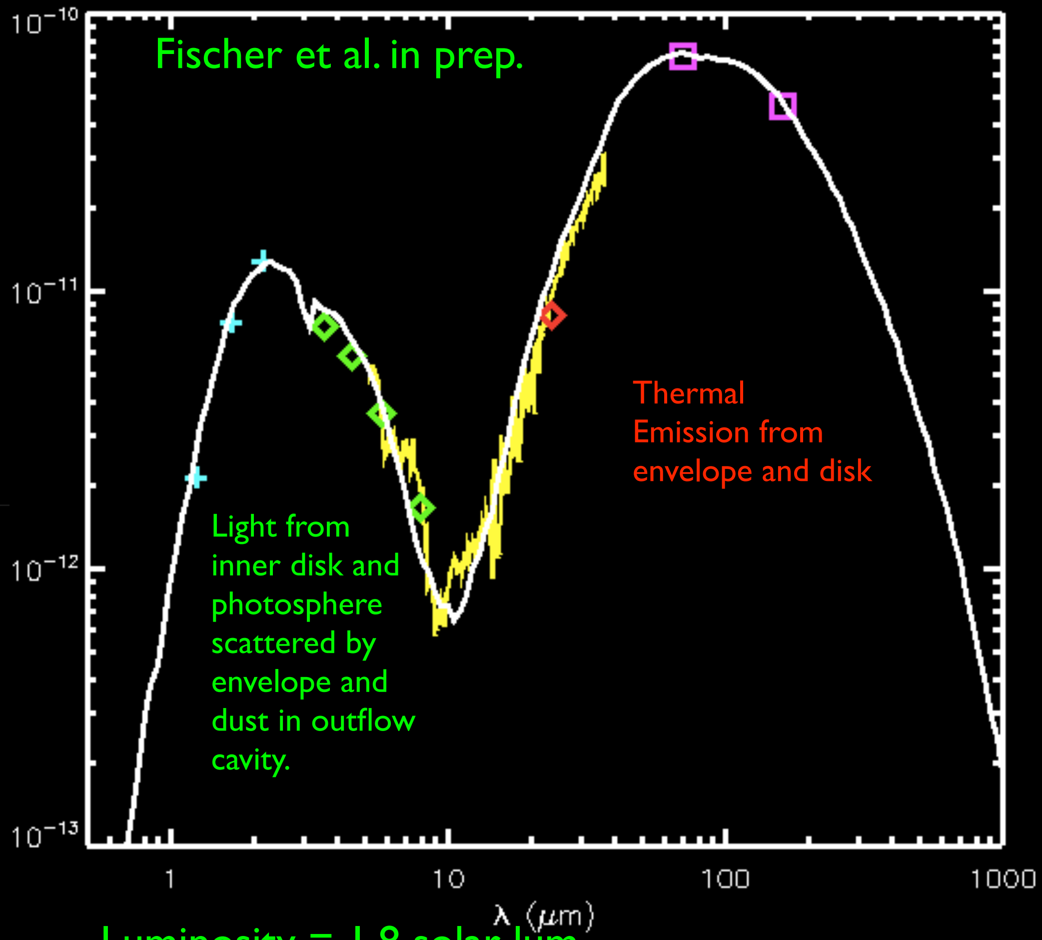

Fischer et al. in prep.

Light from inner disk and photosphere scattered by envelope and dust in outflow cavity.

Thermal Emission from envelope and disk

Luminosity = 1.8 solar lum.

Mass infall = 3x10^{-6} solar masses per year

Rc = 500 AU

Inclination = 90° (opposed to 81° from Robitaille fitter)

“Rainfall” from protostellar envelopes onto protoplanetary disks

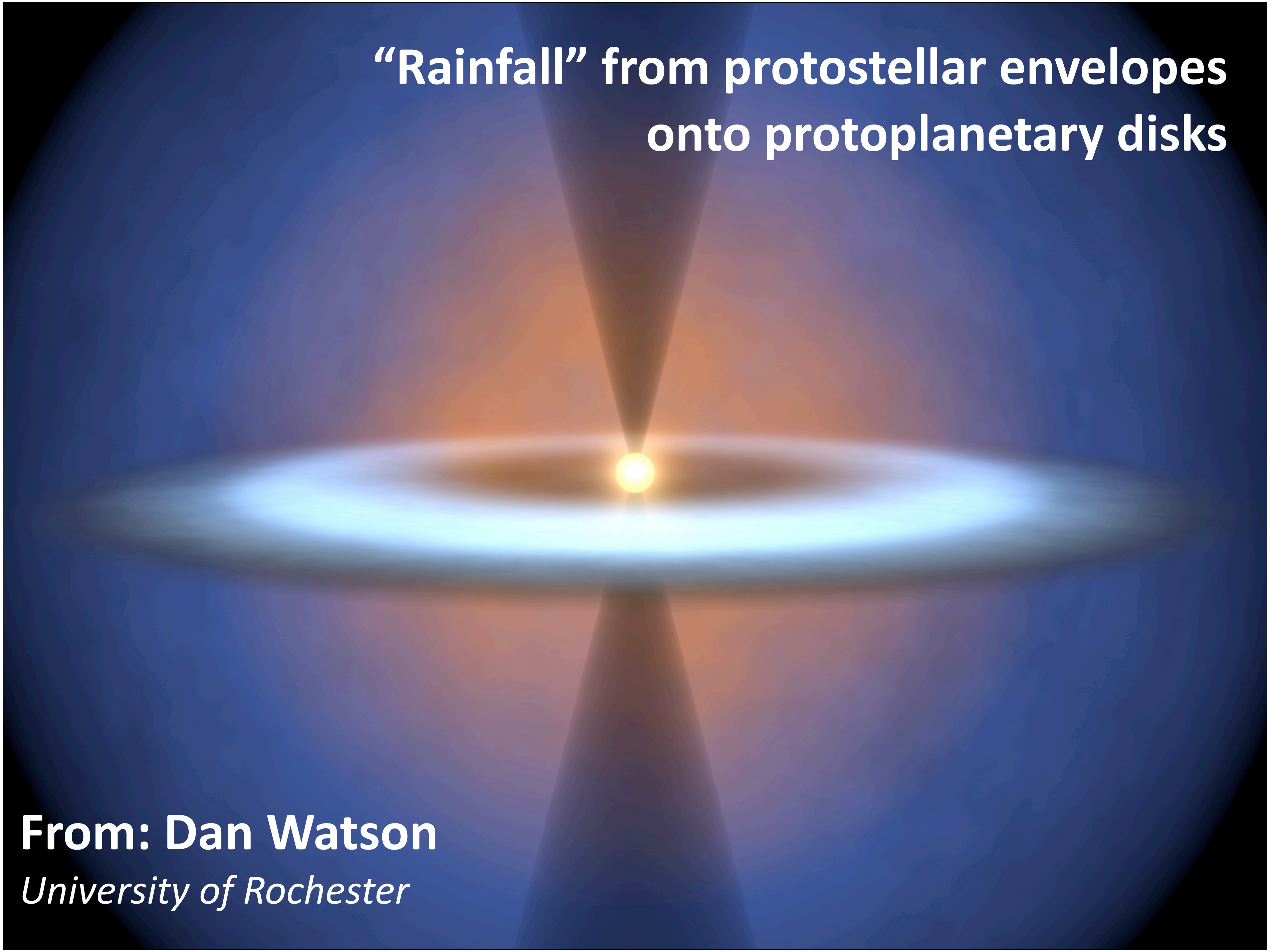

From: Dan Watson

University of Rochester

Spitzer-IRS observations of

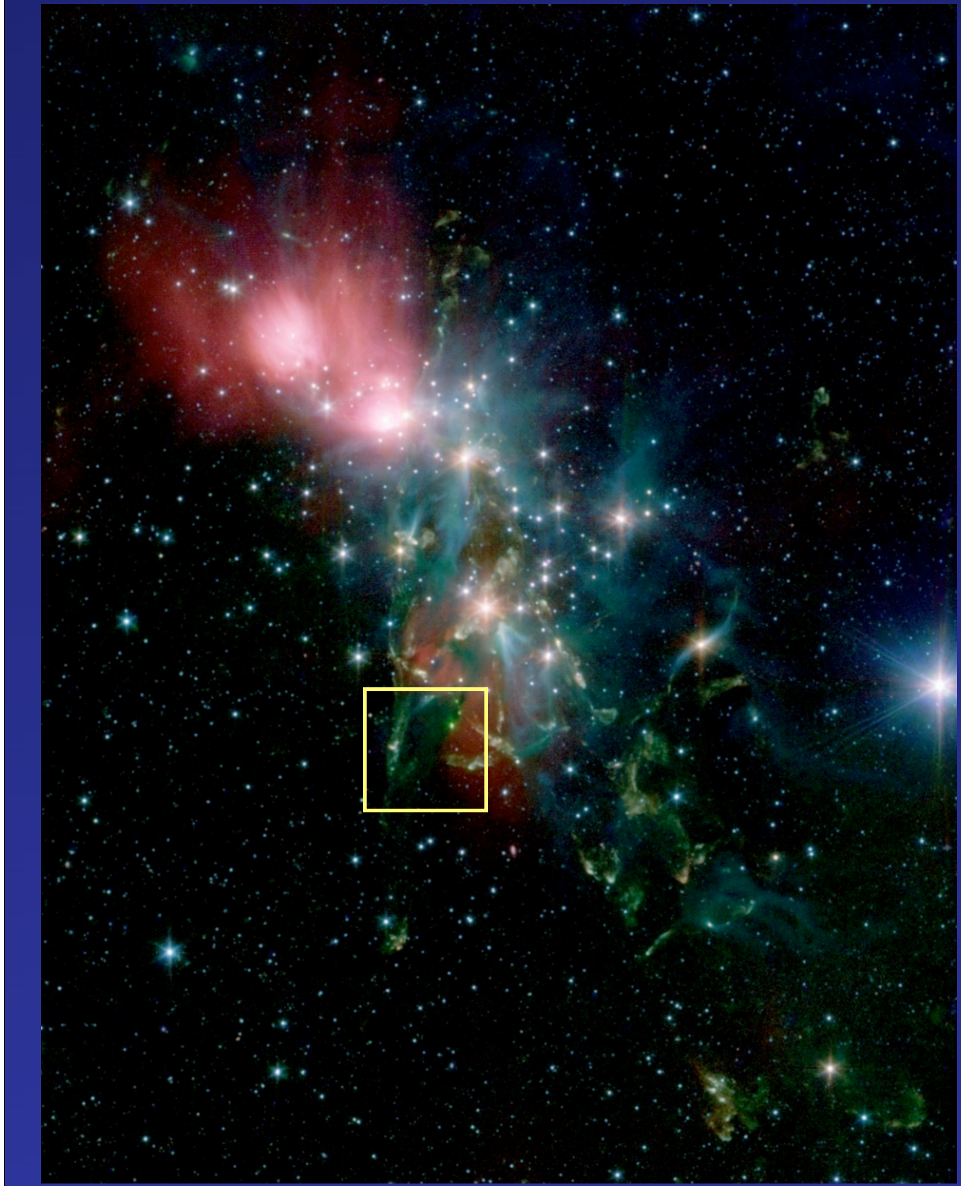

IRAC image: *BGR* = 3.5, 4.5, 8 μm

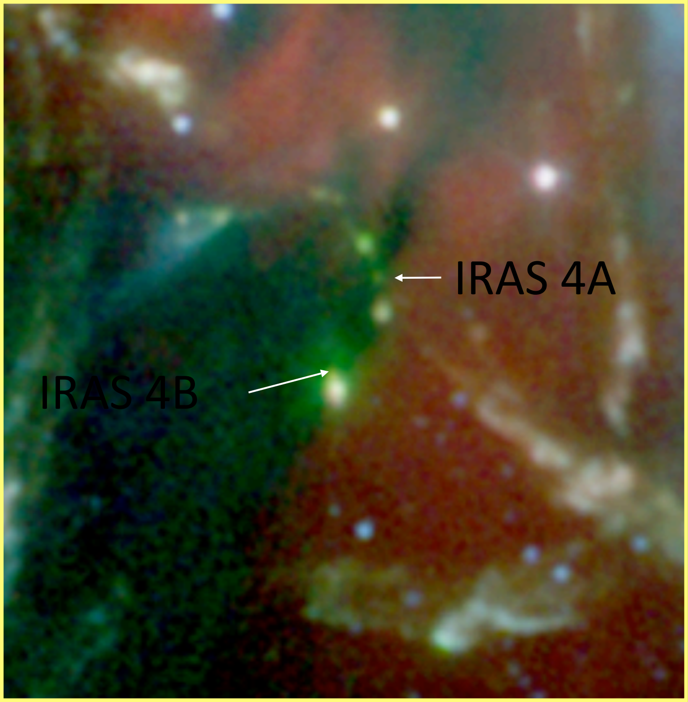

(courtesy of Rob Gutermuth)

A Face on Protostar

NGC 1333 IRAS 4B:

- Possessor of a angularly-compact high-velocity outflow: *projected* length only about 10^4 AU.
- Near a streak of faint near-infrared emission that resembles light scattered from the inner surface of an outflow cavity.
- Thus we view it nearly face on. It is the only one of the first 30 that is viewed in this way.
- Infall observed kinematically in envelope: $\dot{M} = 10^{-4} M_{\odot}\ \mathrm{yr}^{-1}$.

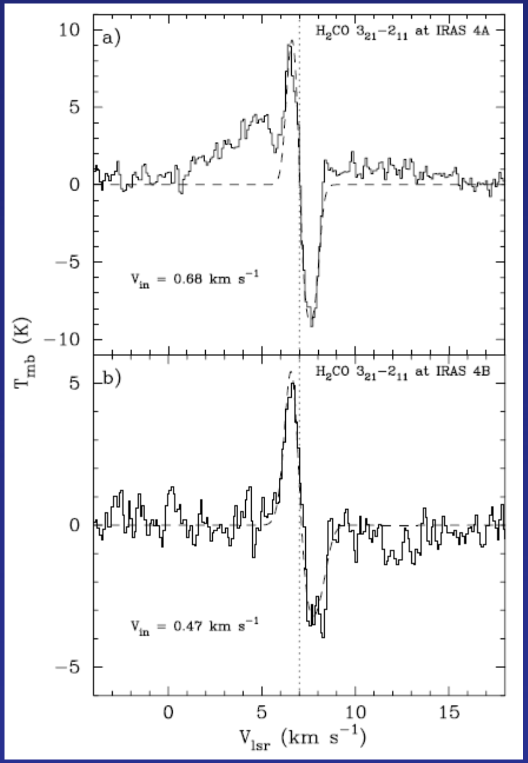

Redshifted absorption toward NGC 1333 IRAS4A and IRAS4B (di Francesco et al. 2001).

Water and OH emission observed in

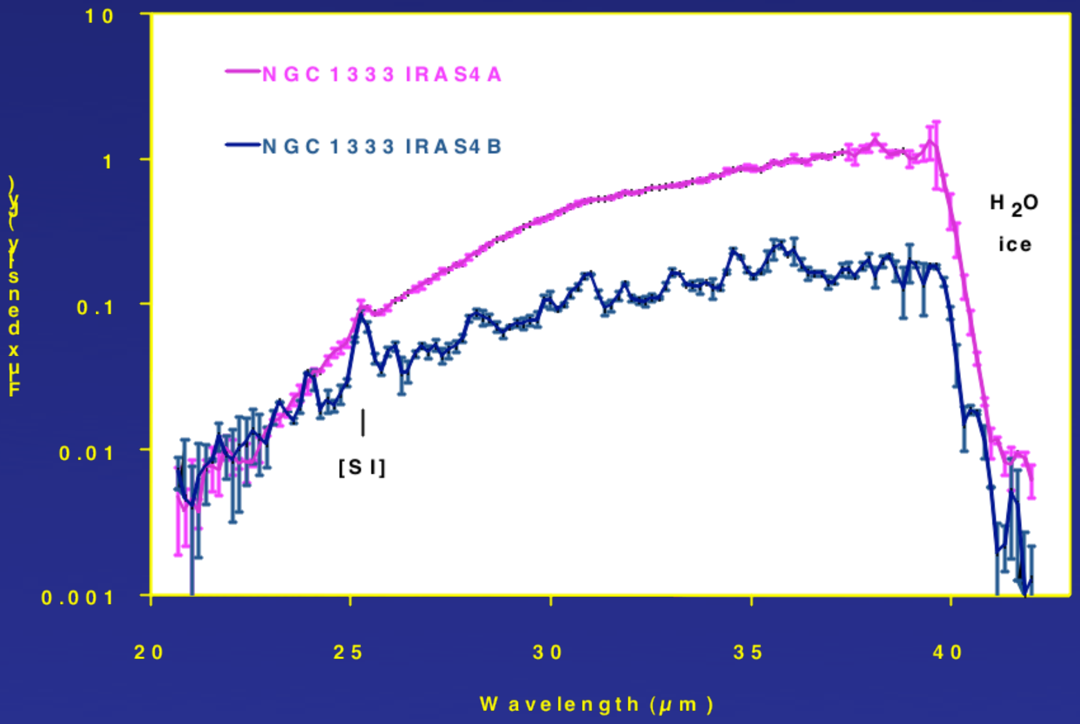

IRS, low spectral resolution

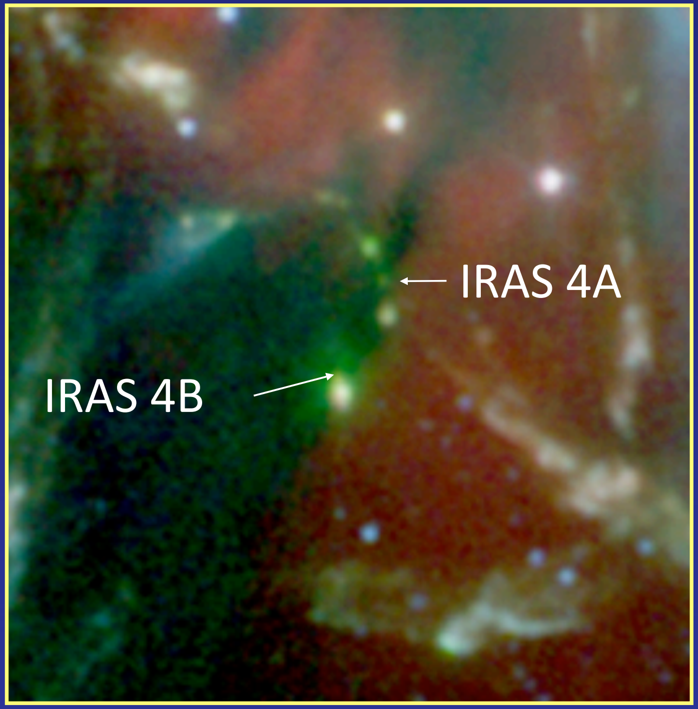

Both IRAS 4A and IRAS 4B have [S I] emission (from their outflows), but IRAS 4B also has broad features coincident with collections of strong transitions of **water**.

Watson et al. 2007

Water and OH emission observed in

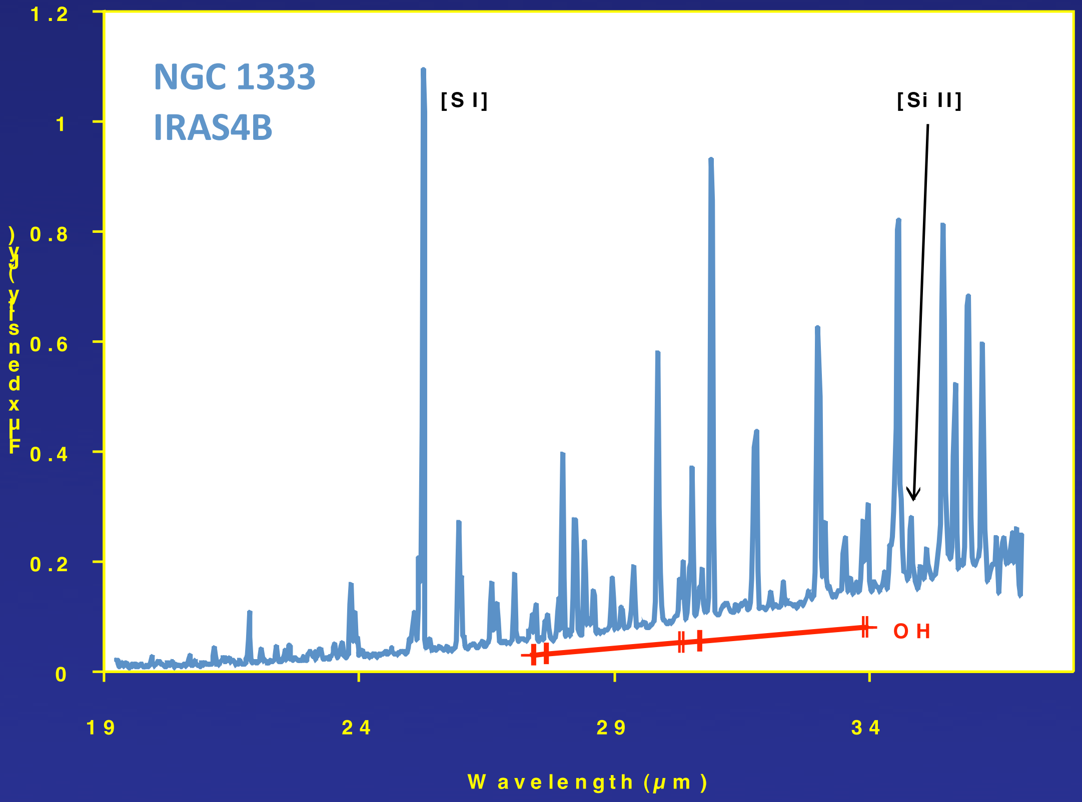

IRS, high spectral resolution

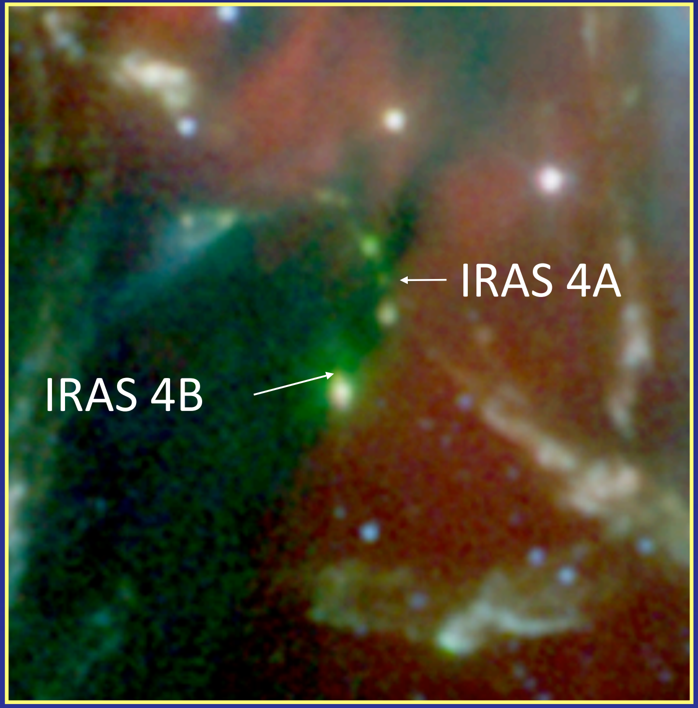

Besides [S I] and [Si II]: >90 rotational transitions of $H_2{}^{16}O$ seen alone or in unresolved combinations, five lines of $H_2{}^{17}O$ or $H_2{}^{18}O$, and 10 rotational lines of ^{16}OH, in IRAS 4B.

Watson et al. 2007

Water and OH emission observed in

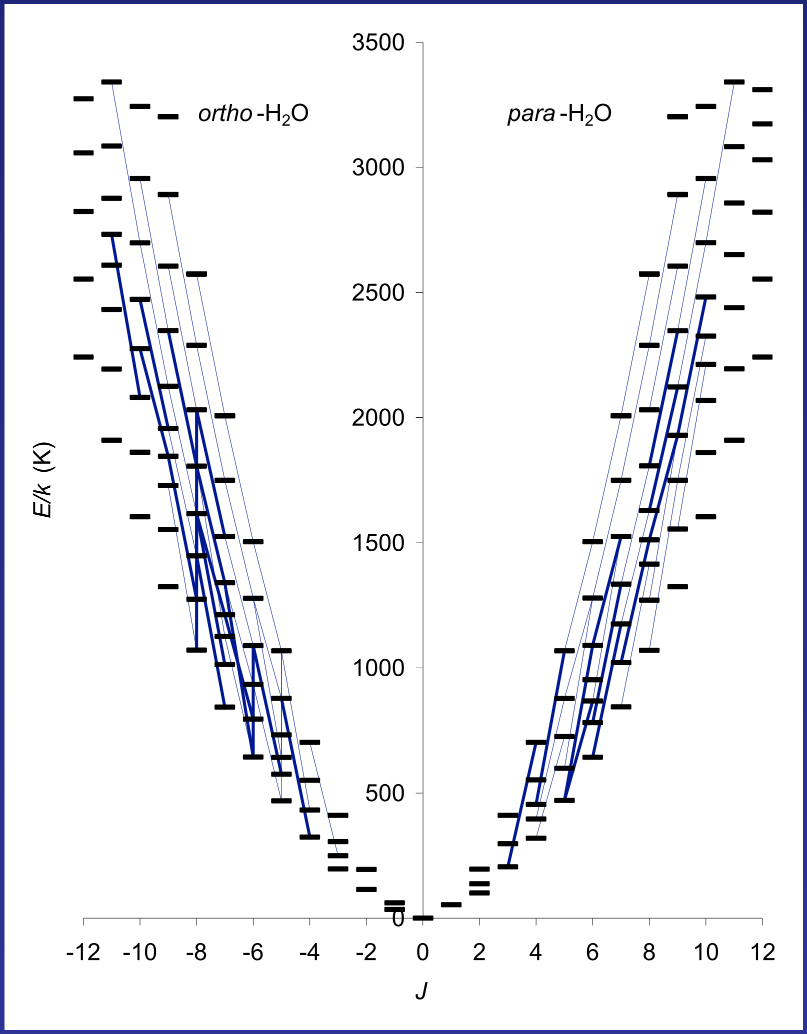

Water transitions detected in IRAS 4B

- All lines from lowest vibrational state: the emission is not fluorescence.
- Upper states: critical densities for collisional de-excitation in the range 10^{10}-10^{13} cm^{-3}, so the gas is *very* dense.
- Collisional rate coefficients have never been computed for 40% of the detected water lines, or *any* of the detected OH lines.
- Wavelengths and excitation distributed: hotter material is not more heavily extinguished.

Watson et al. 2007

The physical condition of the water in NGC

Simple model works well for the water emission lines, OK for OH.

- ❑Assumed: plane-parallel LVG, escape probability, LTE, screen.

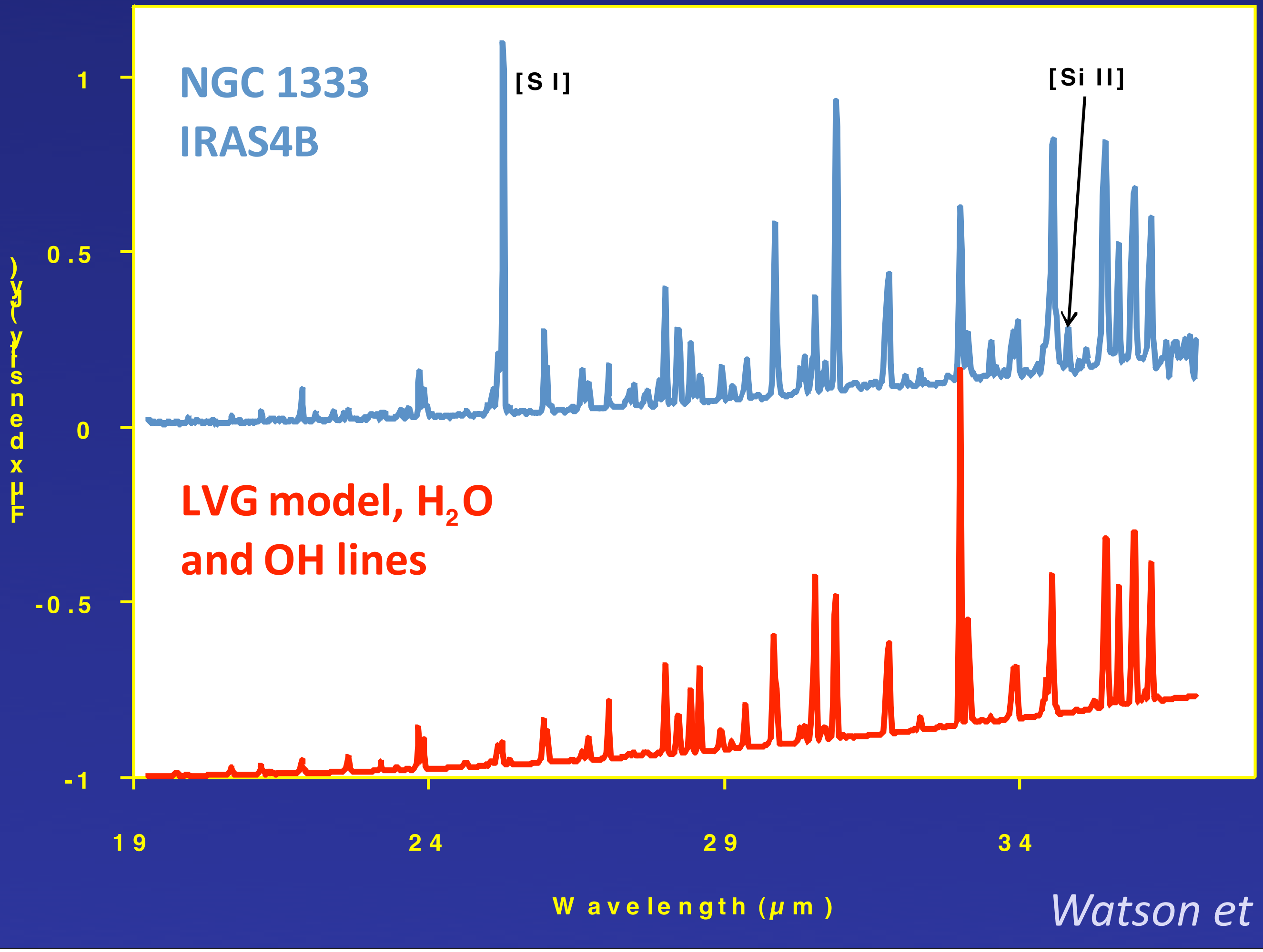

Watson et al. 2007

The physical condition of the water in NGC

According to the model:

- Brightest water lines have $\tau \sim 10$ (i.e. fairly optically thick), but most water lines and all OH lines are optically thin.
  - Thus the **column density *N*** can be determined separately from the optically-thin line fluxes, giving Δv in turn.
  - Thus the **area of the emitting region** can be determined separately from the optically-thick line fluxes and *T*.
- The total power in the water lines we detect is about a third of the total luminosity emitted by water in the object; we thus get an accurate estimate of the **total molecular cooling luminosity**.
  - Rotational water lines are very likely to be the dominant coolant of the gas (Neufeld and Kaufman 1993, Neufeld and Hollenbach 1994).
  - Nevertheless, significant cooling by dust is possible.

The physical condition of the water in NGC

Gas density	Thermal equilibrium, requiring $n(H_2) > 10^{10}$ cm^{-3}
Gas temperature	170 K
Extinction by envelope	$A_V = 100$, interstellar-like
H_2O column density	9.2×10^{16} cm^{-2}
H_2O-line-emitting mass	3.8×10^{24} gm (H_2O) ~3×10^{27} gm (total)
Emitting area	6000 AU^2
Velocity linewidth	2 km sec^{-1}
Total H_2O-line luminosity	$0.03L_\odot$ (extinction-corrected)
OH/H_2O	~0.01
$H_2{}^{18}O/H_2{}^{16}O$	1/590
$H_2{}^{17}O/H_2{}^{16}O$	~1/1500
Envelope dust temperature	59 K

Very dense

Not very hot

~3 Earth oceans

Solar-system size

Very uncertain; OH states far from LTE population

Watson et al. 2007

Protostellar “rain” (continued)

Disk accretion shock model summary for NGC 1333 IRAS4B:

Envelope-disk accretion rate	$0.7\times10^{-4}\ M_\odot\ \mathrm{year}^{-1}$
Shock speed	$2\ \mathrm{km\ sec}^{-1}$
H_2O-line-emitting mass, both faces of disk	7.5×10^{24} gm (H_2O) $\sim6\times10^{24}$ gm (total)
Shocked area	$6000\ \mathrm{AU}^2$, each face
Dimensions of shock	Annulus, r = 40-60 AU
Protostar mass (if it dominates the gravity)	$0.14M_\odot$

Watson et al. 2007

Consistent with envelope infall rate.

Consistent with LVG model linewidth.

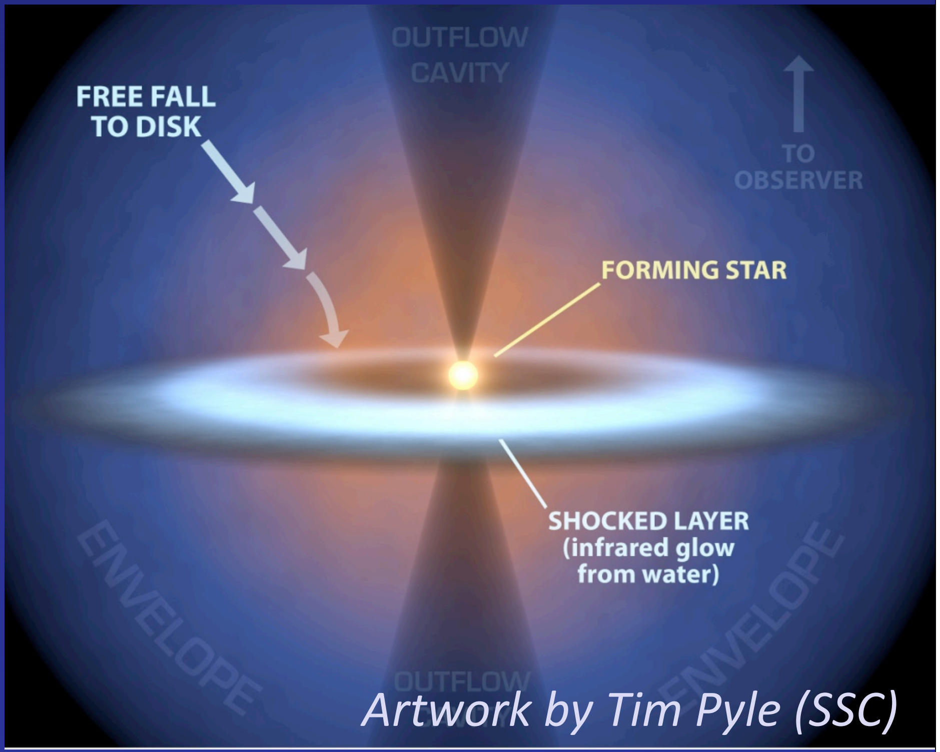

Artwork by Tim Pyle (SSC)

Disk assembly and the state of water on arrival

Thus we see that in Class 0 objects, envelopes fall supersonically onto the future planet-forming region of embedded, new protoplanetary disks, at rates up to $\sim 10^{-4} M_{\odot}$ year^{-1}.

- Face-on ones; in others extinction is too large to see the disk.
- This is our first view of protostellar envelope-disk accretion shocks, and of the protoplanetary-disk assembly process.
  - Such observations yield accurate infall rates, and can give exquisite detail on physical conditions at the disk surface.
- On arrival, the material is heated well above the water-ice sublimation point, and contains both water and OH in substantial abundance.
  - Thus, although water falls as ice, and returns to ice within the disk, it *arrives* in the protoplanetary system in the form of gas, dense and warm enough to lose any isotopic anomalies rapidly.

Summary

- Rotation and angular momentum modify collapse in significant ways.
- This rotation leads to the formation of disks.
- The rotation also decreases optical depth along rotation axis, allowing light to leak out along.
- Most of the angular momentum is in the disk.
- Material crashing down on disk will create a shock.